Bijections for Baxter Families and Related Objects

Stefan Felsner[*]

Institut für Mathematik,
Technische Universität Berlin.
felsner@math.tu-berlin.de

Éric Fusy [†]

Laboratoire d'Informatique (LIX)
École Polytechnique.
fusy@lix.polytechnique.fr

Marc Noy

Departament de Matemàtica Aplicada II
Universitat Politècnica de Catalunya.
marc.noy@upc.edu

David Orden[‡]

Departamento de Matemáticas
Universidad de Alcalá
david.orden@uah.es

Abstract

The Baxter number B_n can be written as $B_n = \sum_{k=0}^{n} \Theta_{k,n-k-1}$ with

$$\Theta_{k,\ell} = \frac{2}{(k+1)^2\,(k+2)} \binom{k+\ell}{k} \binom{k+\ell+1}{k} \binom{k+\ell+2}{k}.$$

These numbers have first appeared in the enumeration of so-called Baxter permutations; B_n is the number of Baxter permutations of size n, and $\Theta_{k,\ell}$ is the number of Baxter permutations with k descents and ℓ rises. With a series of bijections we identify several families of combinatorial objects counted by the numbers $\Theta_{k,\ell}$. Apart from Baxter permutations, these include plane bipolar orientations with $k+2$ vertices and $\ell+2$ faces, 2-orientations of planar quadrangulations with $k+2$ white and $\ell+2$ black vertices, certain pairs of binary trees with $k+1$ left and $\ell+1$ right leaves, and a family of triples of non-intersecting lattice paths. This last family allows us to determine the value of $\Theta_{k,\ell}$ as an application of the Lemma of Lindström Gessel-Viennot. The approach also allows us to count certain other subfamilies, e.g., alternating Baxter permutations, objects with symmetries and, via a bijection with a class of plane bipolar orientations, also Schnyder woods of triangulations. Most of the enumerative results and some of the bijections are not new. Our contribution is mainly in the simplified and unifying presentation of this beautiful piece of combinatorics.

Mathematics Subject Classifications (2000). 05A15, 05A16, 05C10, 05C78

1   Introduction

This paper deals with combinatorial families enumerated by either the Baxter numbers or the summands $\Theta_{k,\ell}$ of the usual expression of Baxter numbers. Many of the enumeration results have been known, even with bijective proofs. Our contribution to these cases lies in

the integration into a larger context and in simplified bijections. We use specializations of the general bijections to count certain subfamilies, e.g., alternating Baxter permutations, objects with symmetries and Schnyder woods of triangulations.

This introduction will not include definitions of the objects we deal with, nor bibliographic citations, which are gathered in notes throughout the article. Therefore, we restrict it to a kind of commented table of contents.

2 Maps, Quadrangulations, and Orientations 3

Planar maps are defined, as well as subfamilies such as 2-connected maps and quadrangulations. Some combinatorial structures are also defined: plane bipolar orientations for 2-connected maps, and separating decompositions (edge-partitions into 2 non-crossing spanning trees) for quadrangulations. A well-known bijection between 2-connected maps and simple quadrangulations is recalled, which extends to a bijection between plane bipolar orientations and separating decompositions.

3 From Separating Decompositions to Twin Pairs of Binary Trees 6

Separating decompositions induce book embeddings on two pages of the underlying quadrangulation. These special book embeddings decompose into pairs of plane trees. These trees come with a special embedding with the nodes aligned, which we call an alternating layout. The alternating layout is used to define the fingerprint of the tree as a specific binary word. We characterize the pairs of plane trees associated with separating decompositions as those with reversed fingerprints. Such pairs are called twin pairs of plane trees.

4 Bijections for Catalan Families: The Combinatorics of Fingerprints 10

Using a specific embedding of binary trees with the leaves aligned, we define fingerprint and bodyprint for a binary tree. Twin pairs of binary trees are defined as those with reversed fingerprints. The geometric embeddings of plane trees and binary trees are set in correspondence, yielding a bijection between plane trees and binary trees that preserves the fingerprint. This also ensures that twin pairs of plane trees are in bijection with twin pairs of binary trees.

Fingerprint and bodyprint yield a bijection between binary trees with k "left" leaves and ℓ "right" leaves and certain pairs of non-intersecting lattice paths. The Lemma of Lindström Gessel-Viennot allows us to identify their number as the Narayana number $N(k + \ell - 1, k)$.

5 Four Incarnations of Twin Pairs of Trees 14

Twin pairs of binary trees are shown to be in bijection to certain rectangulations and to triples of non-intersecting lattice paths. Via the Lemma of Lindström Gessel-Viennot this implies that there are

$$\Theta_{k,\ell} = \frac{2}{(k+1)^2 \, (k+2)} \binom{k+\ell}{k} \binom{k+\ell+1}{k} \binom{k+\ell+2}{k}.$$

twin pairs of binary trees with $k + 1$ left and $\ell + 1$ right leaves. The bijections of previous sections yield a list of families enumerated by the number $\Theta_{k,\ell}$, including plane bipolar orientations, separating decompositions, 2-orientations of quadrangulations, and rectangulations.

6 Baxter permutations 18

We prove bijectively that $\Theta_{k,\ell}$ counts Baxter permutations with k descents and ℓ rises. The bijections involve the Min- and Max-tree of a permutation and the rectangulations from the previous section. Some remarks on the enumeration of alternating Baxter permutations are added.

The bijections between families counted by $\Theta_{k,\ell}$ have the nice property that they commute with a half-turn rotation. This is exploited to count symmetric structures.

Schnyder woods and 3-orientations of triangulations are known to be in bijection. We add a bijection between Schnyder woods and bipolar orientations with a special property. Tracing this special property through the bijections, we are able to find the number of Schnyder woods on n vertices via Lindström Gessel-Viennot. This reproves a formula first obtained by Bonichon.

2 Maps, Quadrangulations, and Orientations

A *planar map*, shortly called a map, is a connected graph (possibly with loops and multiple edges) embedded in the plane with no edge-crossing. Two maps are considered the same if the embeddings are isotopic. A map M has more structure than a graph, in particular M has *faces*, which are the connected components of the plane split by the embedding. The unique unbounded face is called the *outer face* (also called the infinite face) of M. The edges and vertices are called *outer* or *inner* according to whether they are incident to the outer face or not. An *angle* of M is a triple $a = (v, e, e')$ made of one vertex v and two edges incident to v and consecutive around v. The face in the corresponding sector is the *incident face* of a. A *rooted map* is a map with a distinguished edge, called the *root*, directed so as to have the outer face on its left. The origin of the root is called the *root-origin* and the end of the root is called the *root-end*. A *plane graph* is a rooted map without loops or multiple edges, and a *plane tree* is a plane graph with a unique face.

Definition 2.1. A *plane bipolar orientation* is a pair $O = (M, X)$, where M is a rooted map and X is an acyclic orientation of M, such that the unique source (a vertex with only outgoing edges) is the root-origin s, and the unique sink (a vertex with only incoming edges) is the root-end t. *plane bipolar orientation*

A map is called *2-connected* if it is loopless and has no separating vertex. It is well-known that, if (M, X) is a plane bipolar orientation, then M is 2-connected. Conversely any rooted 2-connected map admits at least one bipolar orientation (this statement holds more generally with "graphs" instead of "maps").

Note.

Plane bipolar orientations yield geometric representations of graphs in various flavors (visibility [43], floor planning [37, 30], straight-line drawing [44, 23]). The thesis of Ossona de Mendez is devoted to studying their beautiful properties and applications [17]; see also [16] for a detailed survey.

A map is *bipartite* if its vertices can be partitioned into black and white vertices such that every edge connects a black vertex with a white vertex. Bipartite plane graphs are always assumed to be endowed with their unique vertex bipartition such that the root-origin is black. Quadrangulations are plane graphs with all faces of degree four. It is well-known that quadrangulations are the *maximal plane bipartite graphs*, that is, any edge-addition either breaks bipartiteness or planarity. *maximal plane bipartite graphs*

Definition 2.2. A *separating decomposition* is a pair $D = (Q, Y)$ where Q is a quadrangulation and Y is an orientation and coloring of the edges of Q with colors red and blue such that:

(1) All edges incident to s are ingoing red and all edges incident to t are ingoing blue.

(2) Every vertex $v \neq s, t$ is incident to a non-empty interval of red edges and a non-empty interval of blue edges. If v is white, then, in clockwise order, the first edge in the interval of a color is outgoing and all the other edges of the interval are incoming. If v is black, the outgoing edge is the clockwise last in its color (see Figure 1).
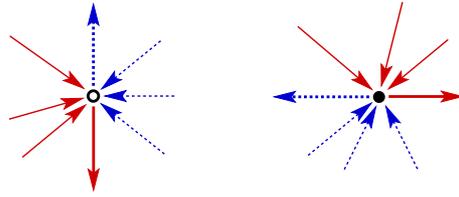
Figure 1: Edge orientations and colors at white and black vertices.

Let M be a rooted 2-connected planar map; the *quadrangulation* of M is the following rooted map Q: The set of vertices of Q is $V_M \cup F_M$, the union of the sets of vertices and faces of M. The edges of Q correspond to incidences between a vertex and a face of M. Note that Q naturally inherits a planar embedding from M; see Figure 2 (ignore the edge orientations and colors here). The faces of Q are in bijection to the edges of M, each face of Q is a quadrangle, hence, Q is a quadrangulation. The 2-connectivity of M implies that Q is a simple graph.

Fix a two-coloring of Q so that the black vertices of Q correspond to the vertices of M and the white vertices of Q correspond to the faces of M. As root-origin of Q choose the root-origin s of M. The root-end of M, which is denoted t, is the vertex opposite to s in the outer face of Q. The two extremities s and t of the root of M are also called the *special vertices* of Q.
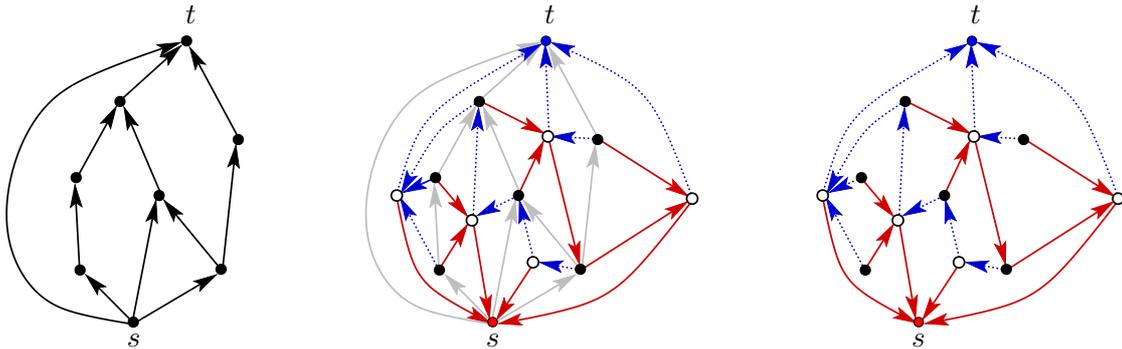
Figure 2: From a plane bipolar orientation to a separating decomposition.

This classical construction can be enriched in order to transfer a plane bipolar orientation $O = (M, X)$ into a separating decomposition of Q. The construction, based on two facts about plane bipolar orientations is illustrated in Figure 2.

Fact V. Every vertex $v \neq s, t$ of G has exactly two angles where the orientation of the edges differ.

Fact F. Every face f of G has exactly two angles where the orientation of the edges coincide.

For every vertex of the quadrangulation Q different from those corresponding to special vertices of M, the facts V and F specify two distinguished edges: On one case, at a vertex $v \neq s, t$ in M we can distinguish the *left* and the *right* of the two special angles. The edge incident to v in Q that corresponds to the left special angle is the outgoing blue edge, the edge that corresponds to the right special angle is the outgoing red edge. On the other case, at a face f of M we have the *source* and the *sink* vertices. The edge in Q between f and the source is the red outgoing edge of the vertex f in Q, and the edge between f and the sink is the blue outgoing edge of f. The rules are illustrated in Figure 3. It is easily verified that they yield a separating decomposition of Q.

Conversely, starting from a given separating decomposition on Q we obtain the unique bipolar orientation on G inducing Q by using the rules backwards: At a vertex v the two outgoing edges of Q split the edges of M into two blocks: the block where Q may have blue edges is the block of incoming edges in the bipolar orientation, the edges of the other block are the outgoing edges in the bipolar orientation. We skip the proof that this indeed yields a bipolar orientation and summarize:
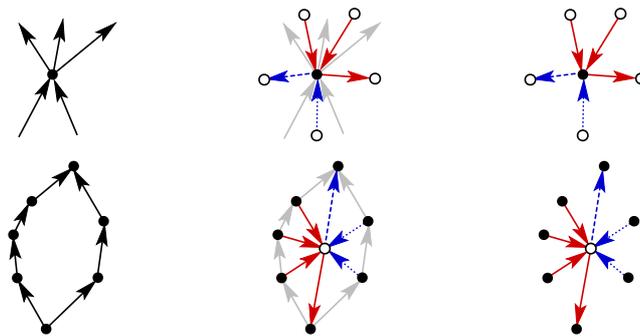

Figure 3: The transformation for a vertex and a face of a rooted map.

Proposition 2.3 (de Fraysseix, de Mendez and Rosenstiehl [16])**.** *Plane bipolar orientations with $\ell + 2$ vertices and $k + 2$ faces are in bijection with separating decompositions with $\ell + 2$ black vertices and $k + 2$ white vertices.*

Note.

The two facts **V** and **F** have been rediscovered frequently, they can be found, e.g., in [16, 37, 43]. Actually, plane bipolar orientations can be defined via properties **V** and **F**. The bijection of Proposition 2.3 is a direct extension of [16, Theorem 5.3].

We end this section with a digression. We show that separating decompositions are just a colorful version of a simpler structure, 2-orientations.

Let Q be a quadrangulation with n faces. Since all faces of Q have degree four, the number of edges of Q is twice the number of faces. Hence, from Euler's relation $|V| - |E| + |F| = 2$, the number of vertices of Q is $n + 2$.

Definition 2.4. An orientation of the edges of a quadrangulation Q is a *2-orientation* if every vertex, except s and t, has outdegree two.

2-orientation

Double-counting the edges of Q ensures that s and t are sinks in every 2-orientation.

Theorem 2.5 (de Fraysseix and de Mendez [14])**.** *Separating decompositions and 2-orientations of a quadrangulation Q are in bijection.*

From the proof we obtain an additional property of a separating decomposition:

(3) The red edges form a tree directed towards s, and the blue edges form a tree directed towards t.

The trees span all of $V \setminus \{s, t\}$ and the respective sinks are s and t.

Note.

De Fraysseix and Ossona de Mendez [14] defined a separating decomposition via properties (1), (2) and (3), i.e., they included the tree-property into the definition. In [14] it is also shown that every quadrangulation admits a 2-orientation.

Proof. Forgetting the coloring, a separating decomposition clearly yields a 2-orientation. For the converse we need to find the color of an edge. Define the *left-right path* of an edge (v, w) as the directed path starting with (v, w) and taking a left-turn in black vertices and a right-turn in white vertices.

left-right path

Claim A. Every left-right path ends in one of the special vertices s or t.

Proof of the claim. Suppose a left-right path closes a cycle. Let C be a simple cycle of a left-right path. Since Q is bipartite the length of C is an even number $2k$. The cycle C has an interior and an exterior. Consider the submap R_C of Q in the interior of C, including C. If r is the number of vertices in the interior of C, then R_C has $r + 2k$ vertices and Euler's formula implies that R_C has $2r + 3k - 2$ edges. However, when we sum up the outdegrees of the vertices we find that k vertices on C contribute 1 while all other vertices contribute 2, which gives a total of $2r + 3k$. This is a contradiction. $\triangle$

Color an edge red if its left-right path ends is s and color it blue if the path ends in t. We show that this coloring obeys the conditions of a separating decomposition.

Claim B. The two left-right paths starting at a vertex do not meet again.

Proof of the claim. Suppose that the two paths emanating from v meet again at w. The two paths form a cycle C of even length $2k$ with r inner vertices. By Euler's formula the inner quadrangulation R_C of C has $2r + 3k - 2$ edges. Split C into the two directed left-right paths B and B' from v to w. From the left-right rule it follows that if all black vertices on B have an edge pointing into the interior of C, then all white vertices on B' have this property. From this it follows that there are at least $k - 1$ edges pointing from C into its interior. Hence, there are at least $2r + 3k - 1$ edges. This is a contradiction. $\triangle$

Consequently, the two outgoing edges of a vertex v receive different colors. It follows that the orientation and coloring of edges is a separating decomposition. $\square$

In Section 8 we use this and some previous bijections to give an independent proof for a beautiful formula of Bonichon [6] for the number of Schnyder woods on triangulations with n vertices.

3 From Separating Decompositions to Twin Pairs of Binary Trees

An embedding of a graph is called a *2-book embedding* if the vertices are arranged on a single

2-book embedding

line so that all edges are either below or above the line. As we show next, a separating decomposition S easily yields a 2-book embedding of the underlying quadrangulation Q.

Define a *bicolored angle* of S as an angle of Q delimited by two edges of different colors (one red and one blue). With a little case analysis (working with the rules given in Definition 2.2) one easily shows that each inner face f of Q has exactly two bicolored angles. Define the *separating curve* for f as a simple curve inside f connecting the two vertices incident to the bicolored angles of f. Define the *equatorial line* L of S as the union of all separating curves of inner faces. The definition of a separating decomposition implies that each inner vertex of Q has degree two in the equatorial line, while s and t have degree zero and the two white vertices of the outer face have degree one (see Figure 4). This implies that the equatorial line is the vertex-disjoint union of a path and possibly a collection of cycles spanning all the vertices in $V \setminus \{s, t\}$.

equatorial line

Lemma 3.1. *Given a quadrangulation Q endowed with a separating decomposition S, the equatorial line of S consists of a single path that traverses every inner vertex and every inner face of Q exactly once. In addition, L separates the blue and the red edges.*

Proof. Assume that the equatorial line L has a cycle C. Consider a plane drawing of $Q \cup C$. The cycle C splits the drawing into an inner and an outer part, both special vertices s and t being in the outer part. The red edges of all vertices of C emanate to one side of C while the blue edges go to the other side. Therefore, it is impossible to have a monochromatic path from a vertex $v \in C$ to both special vertices. With property (3) of separating decompositions, it thus follows that there are no cycles, so the equatorial line is a single path. We have already noted that L spans all the vertices in $V \setminus \{s, t\}$ and traverses every inner face. The result follows. $\qquad\square$

To produce a 2-book embedding, stretch the equatorial line as a straight horizontal line such that the lower halfplane contains all red edges and the upper one contains all blue edges of S. This can be done with a homeomorphism of the plane, so that the drawing remains crossing-free. Finally use another homeomorphism to move s and t onto the equatorial line so that s is the leftmost vertex and t is the rightmost one on the line; see Figure 4, where the equatorial line is represented by the crooked curve in the left picture.
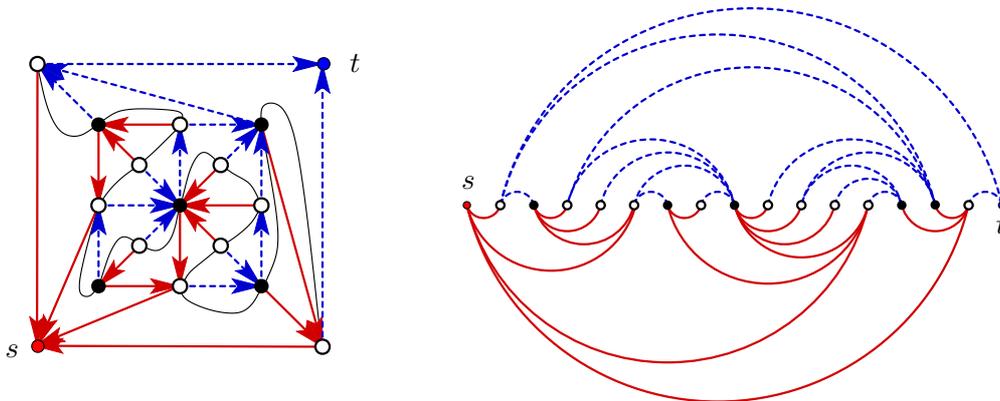

Figure 4: A quadrangulation Q with a separating decomposition S, and the 2-book embedding induced by the equatorial line of S.

Definition 3.2. An *alternating layout* of a plane tree T with $n + 1$ vertices is a non-crossing drawing of T such that its vertices are placed at different points of the x-axis and all edges are embedded in the halfplane above the x-axis (or all below). Moreover, for every vertex v it holds that all its neighbors are on one side, either they are all left of v or all right of v. In these cases we call the vertex v respectively a *right* or a *left vertex* of the alternating layout. Finally, the root-origin and the root-end have to be the two extremal points on the axis. *alternating layout*

right
left vertex

An alternating layout of a plane tree is uniquely determined by the placement of the root-origin (left/right) and the choice of a halfplane for the edges (above/below). We denote the four choices with symbols, e.g., $\diagup$ denotes that the root-origin is left and the halfplane below; the symbols $\diagdown$, $\diagup$ and $\diagdown$ represent the other three possibilities. By induction on the height, one easily shows that if the root-origin is at the left extremity then all vertices at even height (colored black) are left and all vertices at odd height (colored white) are right. And similarly if the root-origin is at the right extremity then the vertices at even height are right and the vertices at odd height are left.

By convention, if the four outer vertices of a quadrangulation in clockwise order are (s, v, t, v'), then the blue tree has root-origin t and root-end v, and the red tree has root-origin s and root-end v'.

Proposition 3.3. *The 2-book embedding induced by a separating decomposition yields simultaneous alternating layouts of the red tree and the blue tree, that are respectively $\diagup$ and $\diagup$.*

Proof. This follows directly by induction on the height of each tree, using the local rules in Definition 2.2. See also Figure 4 for an example. $\qquad\square$

Note.

A proof of Proposition 3.3 was given by Felsner, Huemer, Kappes and Orden [20]. These authors study what they call *strong binary labelings of the angles of a quadrangulation.* They show that these labelings are in bijection with 2-orientations and separating decompositions. In this context they find the 2-book embedding; their method consists in ranking each vertex v on the spine of the 2-book embedding according to the number of faces in a specific region $R(v)$. The original source for a 2-book embedding of a quadrangulation is [15], by de Fraysseix, Ossona de Mendez and Pach. General planar graphs may require as many as four pages for a book embedding, Yannakakis [45].

Alternating layouts of plane trees in our sense were studied by Rote, Streinu and Santos [38] as *non-crossing alternating trees.* Gelfand et al. [26] call this class of trees *standard trees*; they show that these trees are a Catalan family. In [38] connections with rigidity theory and the geometry of the associahedron are established.

As we have seen a separating decomposition yields a pair of plane trees, but, which pairs of trees arise this way? To answer this question we introduce the notion of fingerprints. The full answer to this question is given below in Theorem 3.6. As far as we know this theorem is new. It has the merit of translating problems on 2-orientations into problems on two not too dependent trees.

The unique $\diagup$-alternating layout of T, is obtained by starting at the root and walking clockwise around T, thereby numbering the vertices with consecutive integers according to the following rules: The root is numbered 0 and all vertices in the color class of the root

receive a number at the first visit while the vertices in the other color class receive a number at the last visit. Figure 5 shows an example. Rules for the other types of alternating layouts are:

$\nwarrow$-layout: walk counterclockwise, root class at first visit, other at last visit.

$\nearrow$-layout: walk counterclockwise, root class at last visit, other at first visit.

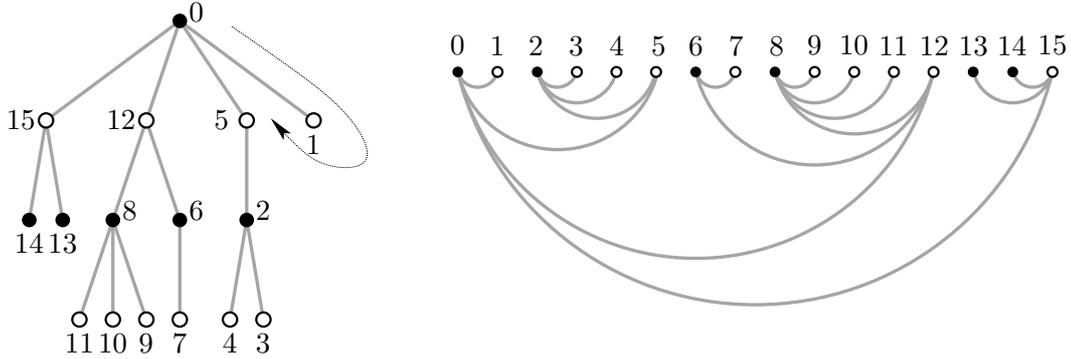$\searrow$-layout: walk clockwise, root class at last visit, other at first visit.

Figure 5: A tree, the numbering and the $\nearrow$-alternating layout.

The $\nearrow$-*fingerprint*, denoted $\alpha_{\nearrow}(T)$, of a rooted plane tree T, is a $0,1$ string which has a 1 at position i ($\alpha_i = 1$) if the ith vertex in the $\nearrow$-alternating layout of T is a left vertex; otherwise, if the vertex is a right vertex then $\alpha_i = 0$. The $\nearrow$-fingerprint of the tree T from Figure 5 is $\alpha_{\nearrow}(T) = 1010001010000110$. Other types of fingerprints are defined by the same rule. For example the $\nearrow$-fingerprint of the tree in Figure 5 is $\alpha_{\nearrow}(T) = 1001111010111010$. With the numbering from Figure 5 this corresponds to the vertex order $15, 14, 13, 12, 11, 10, 9, 8, 7, 6, 5, 4, 3, 2, 1, 0$.

In any of the four layouts, the first vertex is a left vertex and the last one a right vertex. Therefore, a fingerprint has always a 1 as first entry and a 0 as last entry. A *reduced fingerprint* $\hat{\alpha}_{\nearrow}(T)$ of a tree T is obtained by omitting the first and the last entry from the corresponding fingerprint. For a $0,1$ string s we define $\rho(s)$ to be the reverse string and $\bar{s}$ to be the complemented string. For example: if $s = 11010$, then $\rho(s) = 01011$, $\bar{s} = 00101$, and $\overline{\rho(s)} = \rho(\bar{s}) = 10100$.

Lemma 3.4. *For every tree T one has $\alpha_{\nearrow}(T) = \overline{\rho(\alpha_{\nearrow}(T))}$ (and $\alpha_{\nwarrow}(T) = \overline{\rho(\alpha_{\searrow}(T))}$).*

Proof. Take the $\nearrow$-alternating layout of T and rotate it by 180°. This results in the $\nearrow$-alternating layout. Observe what happens to the fingerprint. $\square$

Definition 3.5. A pair (S, T) of rooted, plane trees whose reduced fingerprints satisfy $\hat{\alpha}_{\nearrow}(S) = \overline{\hat{\alpha}_{\nearrow}(T)}$, or equivalently $\hat{\alpha}_{\nearrow}(S) = \rho(\hat{\alpha}_{\nearrow}(T))$, is called a *twin pair of plane trees*.

Theorem 3.6. *There is a bijection between twin pairs of plane trees (S, T) on n vertices and separating decompositions of quadrangulations on $n + 2$ vertices.*

Proof. The mapping from separating decompositions on $n + 2$ vertices to twin pairs of plane trees was already indicated. To recapitulate: a separating decomposition yields a 2-book embedding (Proposition 3.3). The 2-book embedding induces a simultaneous alternating

9

layout of the red tree S^+ and the blue tree T^+. Every non-special vertex $v \neq s, t$ is a left vertex in one of the trees S^+ and T^+ and right vertex in the other one (Proposition 3.3). In terms of fingerprints this reads $\alpha_\swarrow(S^+) + 0 = \overline{1 + \alpha_\nearrow(T^+)}$. Trees S and T are obtained by deleting the left child of the root in S^+ and the right child of the root in T^+; they are both leaves and correspond to the two non-special outer vertices of Q. Since trees S and T satisfy $\hat\alpha_\swarrow(S) = \overline{\hat\alpha_\nearrow(T)}$, (S, T) is a twin pair of plane trees.

The inverse map is illustrated with an example in Figure 6. Let (S, T) be a twin pair of plane trees. Augment both plane trees S and T by a new vertex, which is made the rightmost child of the root. Let S^+ and T^+ be the augmented trees, whose vertices at even height are colored black and vertices at odd height are colored weight. Note that $\hat\alpha_\swarrow(S^+) = 0 + \hat\alpha_\swarrow(S)$ and $\hat\alpha_\nearrow(T^+) = \hat\alpha_\nearrow(T) + 1$. Since the first entry of a non-reduced fingerprint is always 1 and the last one is always 0 it follows that $\alpha_\swarrow(S^+) + 0 = \overline{1 + \alpha_\nearrow(T^+)}$.

Consider the $\swarrow$-alternating layout of S^+ and move the vertices in this layout to the integers $0, .., n$. Similarly, the $\nearrow$-alternating layout of T^+ is placed such that the vertices correspond to the integers $1, .., n+1$. At every integer $0 < i < n+1$, a vertex of S^+ and a vertex of T^+ meet. We identify them. As a consequence of the complemented fitting of the fingerprints, a pair of identified vertices are of the same color, hence the graph $Q = S^+ \cup T^+$ is bipartite. Note that every non-special vertex is a left vertex in one of the layouts and a right vertex in the other. Hence, a pair uv can be an edge in at most one of S and T, otherwise u would have a neighbor on its right in both S and T. Thus Q is simple, bipartite and planar. Since Q has $2n$ edges and $n+2$ vertices, it follows from the Euler formula that it has n faces. The count of edge-face incidences implies that Q is a quadrangulation. Finally, the edges of T^+ are colored blue and oriented to the root-origin t of T^+, and the edges of S^+ are colored red and oriented to the root-origin s of S^+. This yields a separating decomposition on Q, with T^+ as blue tree and S^+ as red tree. $\qquad\square$

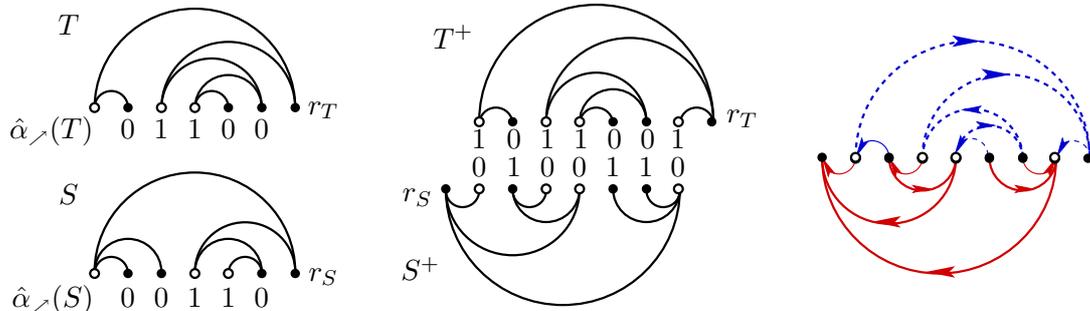
Figure 6: A twin pair of plane trees (S, T). The $\nearrow$-alternating layout of T^+ and the $\swarrow$-alternating layout of S^+ properly adjusted. The induced separating decomposition of a quadrangulation.

4 Bijections for Catalan Families: The Combinatorics of Fingerprints

Vertices of plane trees are partitioned into *leaves* and *inner nodes*, depending on whether the degree is one or greater than one. Let r be the root-origin of a plane tree. In our context

a *binary tree* is a plane tree such that each inner node $v \neq r$ has degree 3 and r has degree 2. In other words, when drawing the tree in a top-to-bottom manner with r at the top, each inner node has two children. The *fingerprint* of a binary tree T is a $0,1$ string which has a 1 at position i if the ith leaf of T is a left child, otherwise, if the leaf is a right child the entry is 0. In Figure 7 the tree T on the right side has $\alpha(T) = 1011101011110010$. The *reduced fingerprint* $\hat{\alpha}(T)$ is obtained by omitting the first and the last entry from $\alpha(T)$. Note that the first entry is always 1 and the last one is always 0.

binary tree

fingerprint

reduced fingerprint

Proposition 4.1. *There is a bijection $T \to B$ which takes a plane tree T with n vertices to a binary tree B with n leaves such that $\hat{\alpha}_{\nearrow}(T) = \hat{\alpha}(B)$.*

Proof. The bijection makes a correspondence between edges of the plane tree and inner nodes of the binary tree; see Figure 7. Embed T with vertices on the integers from 0 to n. With an edge i,j of T associate an inner node x_{ij} for B, which is to be placed at $(\frac{i+j}{2}, \frac{j-i}{2})$. Draw line segments from the vertex $(i,0)$ to x_{ij} and from $(j,0)$ to x_{ij}. Doing this for every edge of T results in a drawing of the binary tree B.
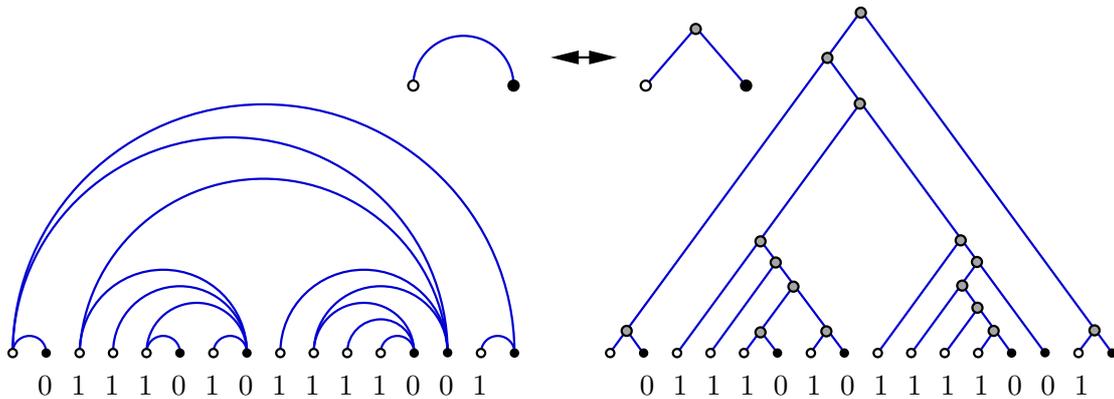

Figure 7: An $\nearrow$- alternating tree T and the binary tree B.

The converse is even simpler. Every inner node x of the binary tree gives rise to an edge connecting the leftmost leaf below x to the rightmost leaf below x. $\square$

Note.

Binary trees with $n+1$ leaves, as well as plane trees with $n+1$ vertices, are counted by the *Catalan number* $C_n = \frac{1}{n+1}\binom{2n}{n}$. Catalan numbers are found in The On-Line Encyclopedia of Integer Sequences [41] as sequence A000108. Stanley [42, Exercise 6.19] collected 66 Catalan families.

Catalan number

Although the subject is well-studied, we include a particular proof showing that binary trees are a Catalan family. Actually, we prove a more refined count related to Narayana numbers. The proof is used later in the context of Baxter numbers.

To start with, we associate another $0,1$ string with a binary tree T. The *bodyprint* $\beta(T)$ is obtained from a visit to the inner nodes of T in in-order; that is $\beta(T) = (\beta(T_L), \beta_x, \beta(T_R))$ when T_L and T_R are the left and right subtrees of the inner node x. The entry of β_x is a 1 if node x is a right-child or it is the root. If the node is a left-child, then $\beta_x = 0$. Note that if the tree T is drawn such that all leaves are on a horizontal line, then there is a one-to-one correspondence between inner nodes and the gaps between adjacent leaves: the gap between

bodyprint

11

leaves v_i and v_{i+1} corresponds to the least common ancestor of v_i and v_{i+1}. Conversely, an inner node x corresponds to the gap between the rightmost leaf in the left subtree of x and the leftmost leaf in the right subtree of x. This correspondence maps the left-to-right order of gaps between leaves to the in-order of inner nodes. Since the root contributes a 1, the last entry of the bodyprint of a tree is always 1. Therefore, it makes sense to define the *reduced bodyprint* $\hat{\beta}(T)$ as $\beta(T)$ minus the last entry. Figure 8 shows an example.

$$\hat{\beta}: \quad 0 \quad 0 \quad 1 \quad 1 \quad 0 \quad 1 \quad 1 \quad 1 \quad 0 \quad 0 \quad 1 \quad 1 \quad 1$$
$$\hat{\alpha}: \quad 0 \quad 1 \quad 1 \quad 1 \quad 0 \quad 1 \quad 0 \quad 1 \quad 1 \quad 1 \quad 1 \quad 0 \quad 0$$
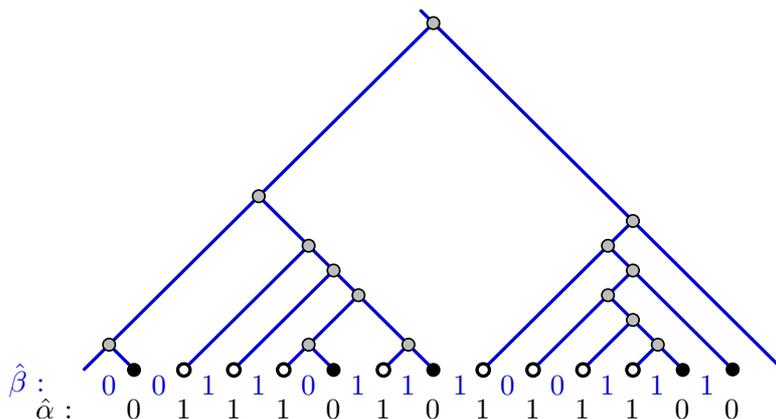
Figure 8: A binary tree with reduced bodyprint $\hat{\beta}$ and reduced fingerprint $\hat{\alpha}$.

Lemma 4.2. *Let T be a binary tree with with k left leaves and $n - k + 1$ right leaves. The reduced fingerprint $\hat{\alpha}(T)$ and the reduced bodyprint $\hat{\beta}(T)$ both have length $n - 1$. Moreover:*

$$(1) \quad \sum_{i=1}^{n-1} \hat{\alpha}_i = \sum_{i=1}^{n-1} \hat{\beta}_i = k - 1 \qquad\qquad (2) \quad \sum_{i=1}^{j} \hat{\alpha}_i \geq \sum_{i=1}^{j} \hat{\beta}_i \quad \text{for all } j = 1, \ldots, n - 1.$$

Proof. Consider a drawing of T where every edge has slope 1 or -1, as in Figure 8. The maximal segments of slope 1 in this drawing define a matching M between the k left leaves, i.e., 1-entries of $\alpha(T)$, and inner nodes which are right-children including the root, i.e., 1-entries of $\beta(T)$. The left part of Figure 9 indicates the correspondence. The reduction $\hat{\alpha}$ (resp. $\hat{\beta}$) has exactly one 1-entry less than α (resp. β). This proves (1).
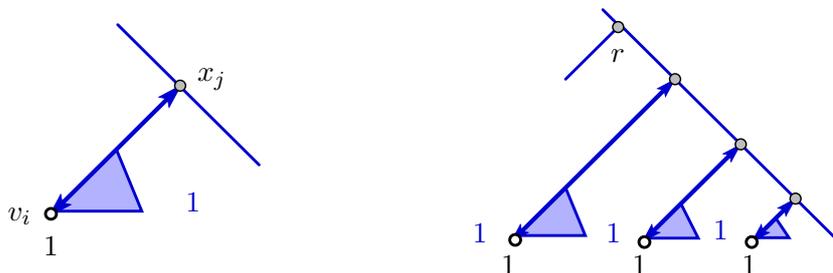

Figure 9: Illustrations for the proof of Lemma 4.2. The pair (v_i, x_j) is in M.

For (2), let $v_0, v_1, \ldots, v_n$ be the set of leaves in left-to-right order and let $x_1, \ldots, x_n$ be the in-order of inner nodes. Note that v_i determines α_i and x_i determines β_i. Let (v_i, x_j) be a pair from the matching M defined above; hence, $\alpha_i = 1$ and $\beta_j = 1$. Since v_i is the leftmost

12

leaf below x_j and the gap corresponding to x_j starts at the rightmost vertex v_{j-1} of the left subtree of x_j, we find that $i \leq j - 1$. This gives a matching between the 1-entries of α and the 1-entries of β, with the property that the index of the 1-entry of α is always less that the index of the mate in β.

To conclude the inequality for the reduced strings we have to address another detail: the mate of the root in M is the leaf v_0, which is not represented in $\hat{\alpha}$, and there is a leaf whose mate in M is the last inner node x_n, which is not represented in $\hat{\beta}$. Consider the ordered sequence $x_{j_0}, x_{j_1}, \ldots, x_{j_s}$ of all vertices on the rightmost branch of T, such that x_{j_0} is the root r and $x_{j_s} = x_n$. The right part of Figure 9 may help to see that in M we have the pairs $(v_0, x_{j_0}), (v_{j_0}, x_{j_1}), \ldots (v_{j_{s-1}}, x_n)$; in particular $\alpha_0 = \alpha_{j_0} = \ldots = \alpha_{j_{s-1}} = 1$ and $\beta_{j_0} = \beta_{j_1} = \ldots = \beta_n = 1$. Hence, we can define a matching M' which is as M except that v_0 and x_n remain unmatched and the pairs (v_{j_i}, x_{j_i}) with $0 \leq i \leq s - 1$ are matched. This matching M' between the 1-entries of $\hat{\alpha}$ and the 1-entries of $\hat{\beta}$ has the property that the index of the 1-entry of $\hat{\alpha}$ is always at most the index of the mate in $\hat{\beta}$. This proves (2). $\qquad\square$

Definition 4.3. Let $\left\langle {n \atop k} \right\rangle$ be the set of cardinality $\binom{n}{k}$ consisting of all 0,1-strings of length n with exactly k entries 1. For $\sigma, \tau \in \left\langle {k+\ell \atop k} \right\rangle$ we say that τ *dominates* σ, denoted $\tau \geq_{\mathsf{dom}} \sigma$, if *dominates* $\sum_{i=1}^{j} \tau_i \geq \sum_{i=1}^{j} \sigma_i$ for all $j = 1, \ldots, n$.

Theorem 4.4. *The mapping $T \leftrightarrow (\hat{\beta}, \hat{\alpha})$ is a bijection between full binary trees with $k + 1$ left leaves and $\ell + 1$ right leaves and pairs $(\hat{\beta}, \hat{\alpha})$ of $0, 1$ strings in $\left\langle {k+\ell \atop k} \right\rangle$ with $\hat{\alpha} \geq_{\mathsf{dom}} \hat{\beta}$.*

Proof. From Lemma 4.2 we know that reduced body- and fingerprint have the required properties. To show that the mapping $T \leftrightarrow (\hat{\beta}, \hat{\alpha})$ is a bijection we use induction.

First note that $\hat{\alpha} = 0^\ell 1^k$ implies $\hat{\beta} = \hat{\alpha}$, and that there are unique trees with these reduced finger- and bodyprints.

If $\hat{\alpha}$ has a different structure, then there is an i such that $\hat{\alpha}_{i-1} \hat{\alpha}_i = 10$. Decompose $\hat{\alpha}(T) = \hat{\alpha}' \, \hat{\alpha}_{i-1} \, \hat{\alpha}_i \, \hat{\alpha}''$ and $\hat{\beta}(T) = \hat{\beta}' \, \hat{\beta}_i \, \hat{\beta}''$ and define $\hat{\alpha}^* = \hat{\alpha}' \, \delta \, \hat{\alpha}''$ and $\hat{\beta}^* = \hat{\beta}' \, \hat{\beta}''$, where $\delta = 1$ if $\hat{\beta}_i = 0$ and $\delta = 0$ if $\hat{\beta}_i = 1$. Depending on the value of $\delta = \overline{\hat{\beta}_i}$, this can be interpreted as either having removed the two entries $\hat{\beta}_i = 1$ and $\hat{\alpha}_{i-1} = 1$ or the two entries $\hat{\beta}_i = 0$ and $\hat{\alpha}_i = 0$ from $\hat{\alpha}$ and $\hat{\beta}$. It is easy to check that $\hat{\alpha}^* \geq_{\mathsf{dom}} \hat{\beta}^*$. By induction there is a unique tree T^* with n leaves such that $(\hat{\beta}(T^*), \hat{\alpha}(T^*)) = (\hat{\beta}^*, \hat{\alpha}^*)$. Making the ith leaf of T^* an inner node with two leaf children yields a tree T with $(\hat{\beta}(T), \hat{\alpha}(T)) = (\hat{\beta}, \hat{\alpha})$.

It remains to show that T is the unique tree with $(\hat{\beta}(T), \hat{\alpha}(T)) = (\hat{\beta}, \hat{\alpha})$. To see this note that in such a tree the leaves v_{i-1}, v_i are a left leaf followed by a right leaf. The leaves v_{i-1} and v_i are children of the inner node x_i, the value $\hat{\beta}_i = 1$ or $\hat{\beta}_i = 0$ depends on whether x_i is itself a left or a right child. Hence pruning the two leaves v_{i-1} and v_i we obtain the tree T^* considered above. $\qquad\square$

An *up-right lattice path* from $(0,0)$ to (ℓ, k), is a path in the square lattice using only steps *up-right* to the right, (addition of $(1,0)$ to the current position) and steps up (addition of $(0,1)$ to *lattice path* the current position). There is a natural correspondence between $0, 1$ strings $\sigma \in \left\langle {k+\ell \atop k} \right\rangle$ and up-right lattice paths from $(0,0)$ to (ℓ, k): it takes an entry 1 into a step to the right and an entry 0 to a step up.

This correspondence yields of a correspondence between pairs $(\sigma, \tau) \in \left\langle {k+\ell \atop k} \right\rangle$ with $\tau \geq_{\mathsf{dom}} \sigma$, and pairs (P_σ, P_τ) of non-intersecting, i.e., vertex disjoint, lattice paths, where P_σ is from $(0,1)$ to $(k, \ell + 1)$ and P_τ is from $(1,0)$ to $(k + 1, \ell)$. This yields a new formulation for Theorem 4.4:

Theorem 4.5. *There is a bijection between binary trees with $k+1$ left leaves and $\ell+1$ right leaves and pairs (P_β, P_α) of non-intersecting up-right lattice paths, where P_β is from $(0,1)$ to $(\ell, k+1)$ and P_α is from $(1,0)$ to $(\ell+1, k)$.*

The advantage of working with non-intersecting lattice paths is that now we can apply the Lemma of Lindström Gessel-Viennot [27].

Theorem 4.6. *The number of binary trees with $k+1$ left leaves and $\ell+1$ right leaves is*

$$\det \begin{pmatrix} \binom{k+\ell}{k} & \binom{k+\ell}{k-1} \\ \binom{k+\ell}{k+1} & \binom{k+\ell}{k} \end{pmatrix} = \frac{1}{k+\ell+1} \binom{k+\ell+1}{k} \binom{k+\ell+1}{k+1}$$

This is the *Narayana number $N(k+\ell+1, k+1)$*. Our bijections imply $\sum_{k=1}^{n-1} N(n,k) = \frac{1}{n}\binom{2n}{n-1} = C_n$; this well-known formula can also be derived as an easy application of Vandermond's convolution. The following proposition summarizes our findings about Narayana families.

Narayana number

Proposition 4.7. *The Narayana number $N(k+\ell+1, k+1)$ counts*

- *plane trees with $k+1$ left vertices and $\ell+1$ right vertices in the alternating layout,*
- *binary trees with $k+1$ left leaves and $\ell+1$ right leaves,*
- *pairs (σ, τ) of $0,1$ strings in $\left\langle \begin{smallmatrix} k+\ell \\ k \end{smallmatrix} \right\rangle$ with $\tau \geq_{\mathsf{dom}} \sigma$,*
- *pairs (P_1, P_2) of non-intersecting up-right lattice paths, where P_1 is from $(0,1)$ to $(k, \ell+1)$ and P_2 is from $(1,0)$ to $(k+1, \ell)$.*

Note.

Narayana numbers can be found in The On-Line Encyclopedia of Integer Sequences [41] as sequence A001263. The Narayana numbers (actually, a q-analogue of them) were first studied by MacMahon [33] and were later rediscovered by Narayana [35]. Stanley [42, Exercise 6.36] recommends to look for decompositions into subsets counted by Narayana numbers in Catalan families. The notion of fingerprints is implicit in Dulucq and Guibert [18]. The combination with the bodyprint and the related bijections are new, according to our knowledge.

5 Four Incarnations of Twin Pairs of Trees

After the Catalan and Narayana digression we now come back to twin pairs of trees. We use the bijections encountered during the digression to give some other interpretations of twin pairs of plane trees.

Definition 5.1. A pair (A, B) of binary trees whose fingerprints satisfy $\hat{\alpha}(A) = \rho(\hat{\alpha}(B))$ is called a *twin pair of binary trees*.

twin pair of binary trees

Theorem 5.2. *There is a bijection between twin pairs of plane trees on n vertices and twin pairs of binary trees with n leaves.*

Proof. Let (A, B) be a twin pair of binary trees. Apply the correspondence from Proposition 4.1 to both. This yields trees S and T such that $\hat{\alpha}_{\nearrow}(S) = \hat{\alpha}(A)$ and $\hat{\alpha}_{\nearrow}(T) = \hat{\alpha}(B)$. From $\hat{\alpha}(A) = \rho(\hat{\alpha}(B))$ we conclude $\hat{\alpha}_{\nearrow}(S) = \rho(\hat{\alpha}_{\nearrow}(T))$ which is the defining property for twin pairs of plane trees. $\square$

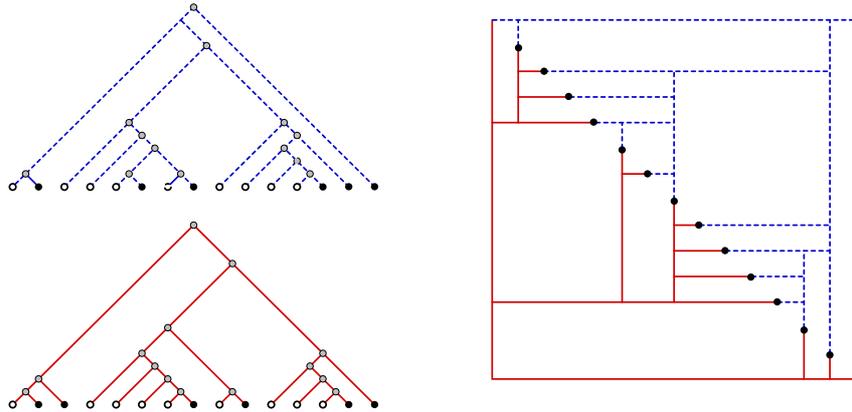The next incarnation of twin pairs of plane trees is in terms of dissections of a square.

14

Figure 10: A twin pair of binary trees and the associated rectangulation.

Definition 5.3. Let X be a set of points in the plane and let R be an axis-aligned rectangle which contains X in its open interior. A *rectangulation of X* is a subdivision of R into rectangles by non-crossing axis-parallel segments, such that every segment contains a point of X and every point lies on a unique segment.

We are mainly interested in rectangulations of diagonal sets, i.e., of the sets $X_{n-1} = \{(i, n-i) : 1 \leq i \leq n-1\}$. In this case the enclosing rectangle R can be chosen to be the square $[0, n] \times [0, n]$.

From a twin pair of binary trees on n vertices we can construct a rectangulation of X_{n-2}: Let (S, T) be a twin pair of binary trees such that both trees are drawn with the same scale, $\pm 45°$ degree slopes, and leaves on the x-axis. Rotate tree T by $180°$ and adjust them such that the leaves match accordingly. This yields a tilted rectangulation of X_{n-2}. Figure 10 shows an example. Conversely, cutting a rectangulation along the diagonal yields a twin pair of binary trees.

The following theorem follows from the above discussion.

Theorem 5.4. *There is a bijection between twin pairs of binary trees with n leaves and rectangulations of X_{n-2}.*

Note.

Hartman et al. [29] and later independently de Fraysseix et al. [15] prove that it is possible to assign a set of internally disjoint vertical and horizontal segments to the vertices of any bipartite map G such that two segments touch if, and only if, there is an edge between the corresponding vertices. A proof of this result can be given along the following lines. From G we obtain a quadrangulation Q by adding edges and vertices. Augment Q with a 2-orientation and trace the mappings from 2-orientations via twin pairs of plane trees to a rectangulation of a diagonal point set. The horizontal and vertical segments through the points are a touching segment representation for Q. Deleting some and retracting the ends of some other segments yields a representation for G. A similar observation was made by Ackerman, Barequet and Pinter [1].

Next, we map twin pairs of binary trees to triples of non-intersecting lattice paths. The map is based on the fingerprint and bodyprint of a binary tree, and the lattice paths associated to them.

15

Recall that the bijection from Theorem 4.5 maps a binary tree T with $k+1$ left and $\ell+1$ right leaves to a pair $(P_\beta(T), P_\alpha(T))$ of non-intersecting up-right lattice paths, where $P_\beta(T)$ is from $(0,1)$ to $(\ell, k+1)$ and $P_\alpha(T)$ is from $(1,0)$ to $(\ell+1, k)$.

A point reflection at $(0,0)$ followed by a translation by $(\ell+2, k)$ maps $(P_\beta(T), P_\alpha(T))$ to the pair $(P_\alpha^*(T), P_\beta^*(T))$ of non-intersecting up-right lattice paths, where $P_\alpha^*(T)$ is from $(1,0)$ to $(\ell+1, k)$ and $P_\beta^*(T)$ is from $(2,-1)$ to $(\ell+2, k-1)$.

Let (S,T) be a twin pair of binary trees with $k+1$ left and $\ell+1$ right leaves. Consider the triple $(P_\beta(S), P_\alpha(S), P_\beta^*(T))$. We know that $P_\beta(S)$ and $P_\alpha(S)$ are non-intersecting. Since by definition $\hat\alpha(S) = \rho(\hat\alpha(T))$, it is easy to see that $P_\alpha^*(T) = P_\alpha(S)$. Therefore, we also know that $P_\alpha(S)$ and $P_\beta^*(T))$ are non-intersecting. Since the first two of these paths uniquely determine S and the last two uniquely determine T we obtain, via a translation of the three paths by one unit up, the following theorem.
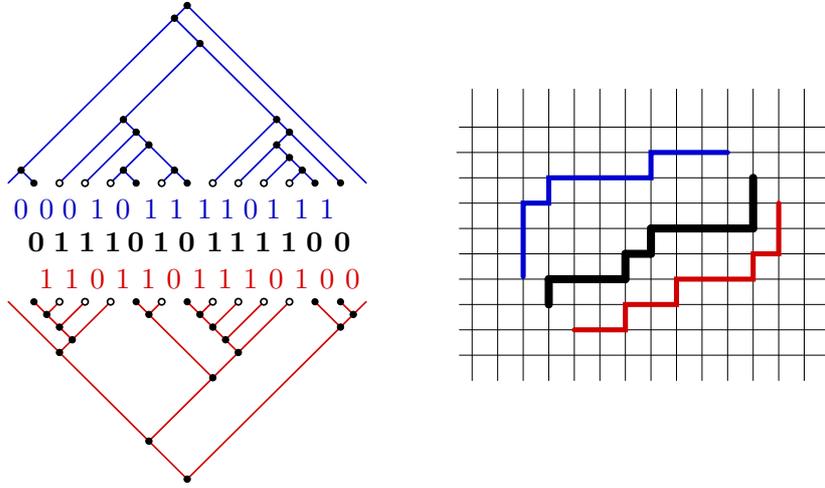

Figure 11: A twin pair of trees binary and its triple of non-intersecting lattice paths. The fingerprint and its path are emphasized.

Theorem 5.5. *There is a bijection between twin pairs of binary trees with $k+1$ left leaves and $\ell+1$ right leaves and triples (P_1, P_2, P_3) of non-intersecting up-right lattice paths, where P_1 is from $(0,2)$ to $(k, \ell+2)$, P_2 is from $(1,1)$ to $(k+1, \ell+1)$, and P_3 is from $(2,0)$ to $(k+2, \ell)$.*

Again we can apply the Lemma of Lindström Gessel-Viennot.

Theorem 5.6. *The number of twin pairs of binary trees with $k+1$ left leaves and $\ell+1$ right leaves is*

$$\det \begin{pmatrix} \binom{k+\ell}{k} & \binom{k+\ell}{k-1} & \binom{k+\ell}{k-2} \\ \binom{k+\ell}{k+1} & \binom{k+\ell}{k} & \binom{k+\ell}{k-1} \\ \binom{k+\ell}{k+2} & \binom{k+\ell}{k+1} & \binom{k+\ell}{k} \end{pmatrix} = 2\,\frac{(k+\ell)!\,(k+\ell+1)!\,(k+\ell+2)!}{k!\,(k+1)!\,(k+2)!\,\ell!\,(\ell+1)!\,(\ell+2)!} = \Theta_{k,\ell}$$

The number $\Theta_{k,\ell}$ has some quite nice expressions in terms of binomial coefficients, e.g., $\Theta_{k,\ell} = \frac{2}{(k+1)^2\,(k+2)}\binom{k+\ell}{k}\binom{k+\ell+1}{k}\binom{k+\ell+2}{k}$ or $\Theta_{k,\ell} = \frac{2}{(n+1)\,(n+2)^2}\binom{k+\ell+2}{k}\binom{k+\ell+2}{k+1}\binom{k+\ell+2}{k+2}$. The total number of twin binary trees with $n+2$ leaves is given by the *Baxter number*

Baxter number

16

$$B_{n+1} = \sum_{k=0}^{n} \Theta_{k,n-k},$$

whose initial values are $1, 2, 6, 22, 92, 422, 2074, 10754$. The next proposition collects families that are, due to our bijections, enumerated by Θ-numbers.

Proposition 5.7. *The number $\Theta_{k,\ell}$ counts*

- *triples (P_1, P_2, P_3) of non-intersecting up-right lattice paths, where P_1 is from $(0,2)$ to $(\ell, k+2)$ and P_2 is from $(1,1)$ to $(\ell+1, k+1)$ and P_3 is from $(2,0)$ to $(\ell+2, k)$.*
- *twin pairs of binary trees with $k+1$ left leaves and $\ell+1$ right leaves,*
- *rectangulations of $X_{k+\ell}$ with k horizontal and ℓ vertical segments,*
- *twin pairs of plane trees with $k+1$ left vertices and $\ell+1$ right vertices in the alternating layout,*
- *separating decompositions of quadrangulations with $k+2$ white and $\ell+2$ black vertices,*
- *2-orientations of quadrangulations with $k+2$ white and $\ell+2$ black vertices.*
- *plane bipolar orientations with $k+2$ faces and $\ell+2$ vertices.*

Note.

In 2001 R. Baxter guessed and checked [4, Eq 5.3] that plane bipolar orientations are counted by the Θ-numbers. His verification is based on algebraic manipulations on generating functions of 2-connected planar maps weighted by their Tutte polynomials.

The concept of twin pairs of binary trees is due to Dulucq and Guibert [18]. They also give a bijection between twin pairs of binary trees and triples of non-intersecting lattice paths. The bijection also uses the fingerprint as the middle path, the other two are defined differently. In [19] they extend their work to include some more refined counts. A very good entrance point for more information about Baxter numbers is The On-Line Encyclopedia of Integer Sequences [41, A001181].

Fusy, Schaeffer and Poulalhon [25] gave a direct bijection from separating decompositions to triples of non-intersecting paths in a grid. Similarly as in this article, they obtain the triple of paths from a triple of words encoding the blue tree and the red tree. However, as opposed to ours, their encoding breaks the symmetry between the blue and the red tree, since they associate two words with the blue tree and one word with the red tree.

Ackerman, Barequet and Pinter [1] also have the result that the number of rectangulations of X_n is the Baxter number B_{n+1}. Their proof is via a recurrence formula obtained by Chung et al. [12]. They also show that for a point set $X_\pi = \{(i, \pi(i)) : 1 \leq i \leq n\}$ to have exactly B_{n+1} rectangulations it is sufficient that π is a Schröder permutation, i.e., a permutation avoiding the patterns $3-1-4-2$ and $2-4-1-3$. They conjecture that whenever π is a permutation that is not Schröder, the number of rectangulations of X_π is strictly larger than the Baxter number.

In contrast to the nice formulas for the number of 2-orientations of quadrangulations on n vertices, very little is known about the number of 2-orientations of a fixed quadrangulation Q. In [22] it is shown that the maximal number of 2-orientations a quadrangulation on n vertices can have is asymptotically between $1,47^n$ and $1,91^n$. To our knowledge, the computational complexity of the counting problem is open.

6   Baxter Permutations

Definition 6.1. The *max-tree* $\mathsf{Max}(\pi)$ of a permutation π is recursively defined. The basis is the unlabeled one-node tree $\mathsf{Max}(\emptyset)$. Otherwise write π as $\pi = \pi_{\mathrm{left}}, z, \pi_{\mathrm{right}}$, where z is the maximum entry of π. Then $\mathsf{Max}(\pi)$ has root labeled z, left subtree $\mathsf{Max}(\pi_{\mathrm{left}})$ and right subtree $\mathsf{Max}(\pi_{\mathrm{right}})$. Figure 12 shows an example.   *max-tree*

The *min-tree* $\mathsf{Min}(\pi)$ is defined similarly but with z being the minimum entry of π.

The max-tree of a permutation is a binary tree. The ith leaf v_i of $\mathsf{Max}(\pi)$ from the left corresponds to the adjacent pair (π_{i-1}, π_i) in the permutation π. Leaf v_i is a left leaf if, and only if, (π_{i-1}, π_i) is a descent, i.e., if $\pi_{i-1} > \pi_i$. A dual characterization holds for $\mathsf{Min}(\pi)$: The ith leaf y_i of $\mathsf{Min}(\pi)$ from the left is a left leaf if, and only if, (π_{i-1}, π_i) is a rise, i.e., if $\pi_{i-1} < \pi_i$.

With these definitions and observations and recalling that $\rho(\pi)$ denotes the reverse permutation of π we obtain:

Proposition 6.2. *For a permutation π of $[n-1]$ the pair $(\mathsf{Max}(\pi), \mathsf{Min}(\rho(\pi)))$ is a pair of twin binary trees.*
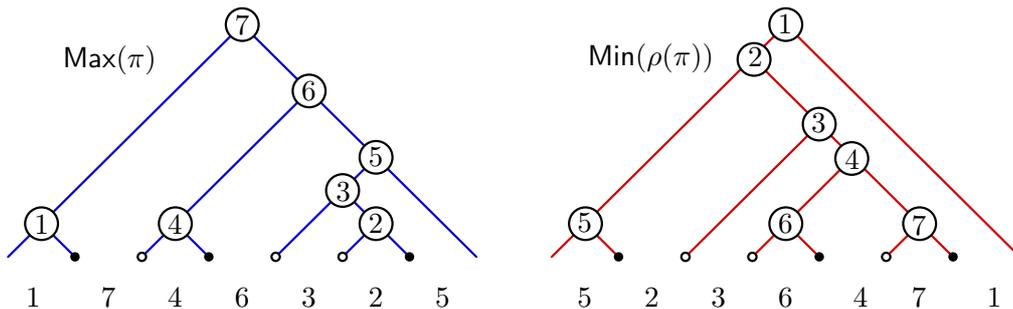

Figure 12: The trees $\mathsf{Max}(\pi)$ and $\mathsf{Min}(\rho(\pi))$ associated with $\pi = 1, 7, 4, 6, 3, 2, 5$.

Identifying a twin pair of binary trees (S, T) with a rectangulation $\mathcal{R}$, it is easy to characterize all permutations π such that $(\mathsf{Max}(\pi), \mathsf{Min}(\rho(\pi))) = (S, T)$. Consider two orders on the rectangles of $\mathcal{R}$: the *left-to-right order* is the total ordering of the rectangles according to their intersections with the x-axis. The *bottom-to-top order*, is the partial order obtained as transitive closure of the relation $\rightarrow$ on rectangles, where $r \rightarrow r'$ iff r and r' are adjacent and r' is either top-right or top-left of r along the adjacency-segment. The bottom-to-top order is denoted $(\mathcal{R}, \leq)$. A *ranking* for $\mathcal{R}$ is a labeling of the n rectangles of $\mathcal{R}$ with distinct labels in $[1..n]$. The rectangle labeled k is denoted $R(k)$. With each ranking one associates the permutation π such that, for $i \in [1..n]$, $\pi(i)$ is the label of the ith rectangle in the left-to-right order. A ranking is called *admissible for $\mathcal{R}$* if it is a linear extension of the bottom-to-top order. Accordingly, permutations associated with admissible rankings are called *admissible permutations for $\mathcal{R}$*, see Figure 13. The permutations that are mapped to $\mathcal{R}$ are exactly the admissible permutations for $\mathcal{R}$.   *left-to-right order*   *bottom-to-top order*   *ranking*   *admissible for $\mathcal{R}$*

The generic procedure to generate admissible rankings for $\mathcal{R}$, i.e., linear extensions of the bottom-to-top order $(\mathcal{R}, \leq)$, is as follows: "At each step i, for i from n to 1, calling $\mathcal{L}$ the set of rectangles already labeled and $\mathcal{U}$ the set of rectangles not labeled, pick a rectangle that is maximal in $(\mathcal{U}, \leq)$ and assign label i to it".
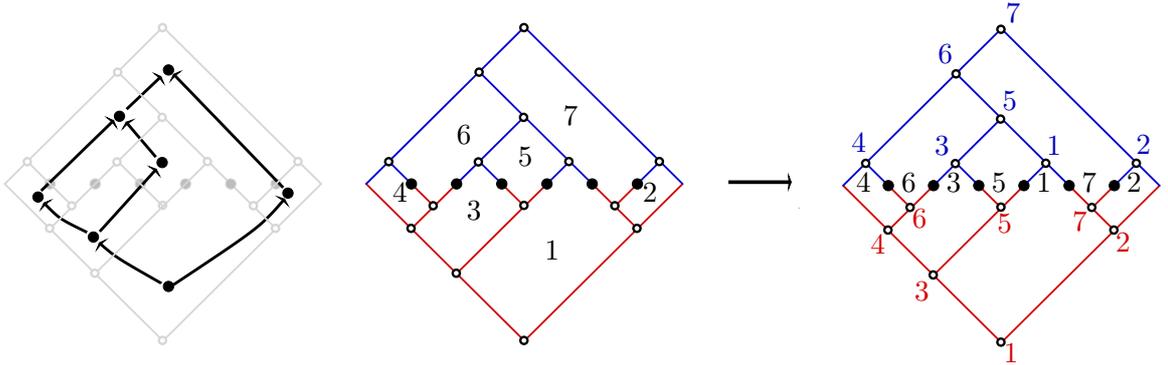
Figure 13: The bottom-to-top relation of a rectangulation $\mathcal{R}$, an admissible ranking of $\mathcal{R}$ and the associated admissible permutation with max- and min-trees.

Definition 6.3. A *Baxter permutation* is a permutation which avoids the pattern 2–41–3 and 3–14–2. That is, π is Baxter if there are no indices $i < j, j + 1 < k$ with $\pi_{j+1} < \pi_i < \pi_k < \pi_j$ nor with $\pi_{j+1} > \pi_i > \pi_k > \pi_j$.

Baxter permutation

Theorem 6.4 (Dulucq and Guibert [18])**.** *There is a bijection between twin binary trees with n leaves and Baxter permutations of $[n-1]$.*

The proof of this theorem actually just requires the proof of one property. Indeed, from the above discussion characterizing the pre-images of a twin pair of binary trees, we just have to show that every rectangulation $\mathcal{R}$ has exactly one admissible permutation that is Baxter. We will show that to generate an admissible Baxter permutation for $\mathcal{R}$ there is a unique choice for the maximal element of $(\mathcal{U}, \leq)$ in each step of the above mentioned generic procedure. This implies that the admissible Baxter permutation for $\mathcal{R}$ is unique.

Definition 6.5. For each step i from n to 1 of the generic procedure generating admissible rankings, the *good rectangle r* is the unique maximal rectangle in $(\mathcal{U}, \leq)$ satisfying the following conditions.

- If $i = n$ then r is the unique maximal rectangle of $(\mathcal{R}, \leq)$.

- If $i < n$ and the south-corner of $R(i+1)$ is a $\curlyvee$ (a left child in tree T), then r is the next maximal element of $\mathcal{U}$ to the left of $R(i+1)$.

- If $i < n$ and the south-corner of $R(i+1)$ is a $\curlywedge$ (a right child in tree T), then r is the next maximal element of $\mathcal{U}$ to the right of $R(i+1)$.

An example for the execution of the procedure with the choice of the good rectangle at each step is shown in Figure 14. In the figure the arrows are placed at the south-corner of the rectangle that was numbered last and point to the direction where the next number is to be placed.

Note that at each step, the boundary between the set $\mathcal{L}$ of already labeled rectangles and the set $\mathcal{U}$ of still unlabeled rectangles is a sequence $s_1, \ldots, s_k$ of segments of slopes alternatively $+1$ or -1, and such that the interior of each segment s_i, $1 \leq i \leq k$, intersects the horizontal axis of the rectangulation $\mathcal{R}$ (calling horizontal axis of $\mathcal{R}$ the line passing by all points of $\mathcal{R}$). This property (easy to show by induction) has to be kept in mind when reading the proofs of the next two lemmas.
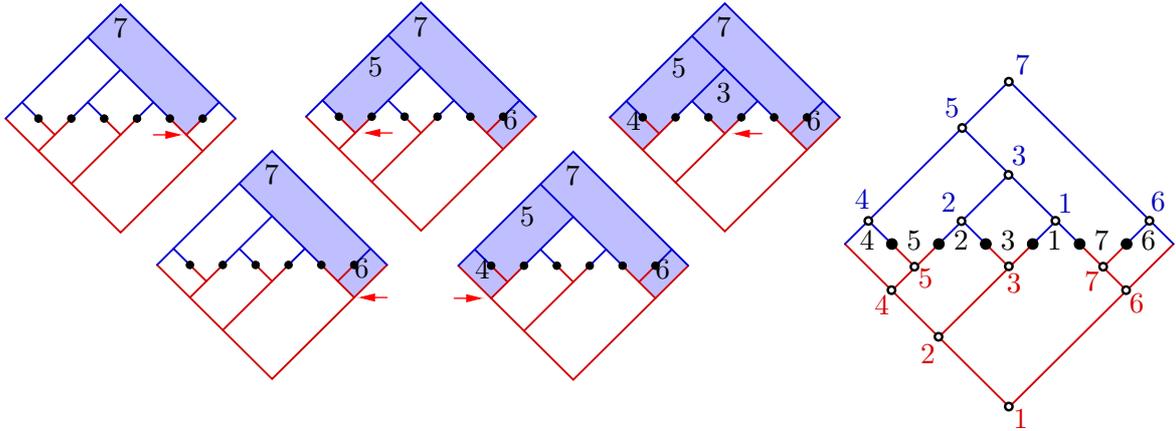
Figure 14: Generating a Baxter permutation from a rectangulation. The final state shows the permutation with its min- and max-trees.

Lemma 6.6. *The choice of the good rectangle at each step yields a Baxter permutation.*

Proof. Let us show that the algorithm does not produce the pattern 2–41–3 (one proves similarly that it does not produce 3–14–2). Let $1 \leq a < b < c < d \leq n$. Going for a contradiction we assume that there are rectangles $R(b)$, $R(d)$, $R(a)$, $R(c)$ in this order from left-to-right, with $R(d)$ immediately to the left of $R(a)$ on the horizontal axis. Choose c minimal with this property and consider the moment at which $R(c)$ gets labeled, see Figure 15 (where p is the south tip of $R(c)$).
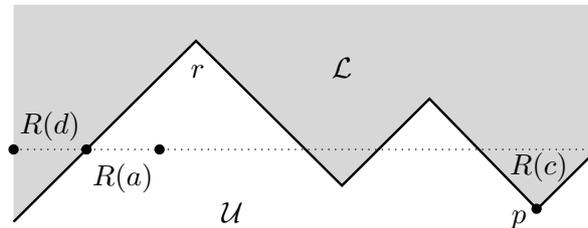

Figure 15: A situation as discussed in the proof of Lemma 6.6.

At that step let $\mathcal{L}$ be the set of already labeled rectangles (rectangles $R(i)$ with $i \geq c$) and $\mathcal{U}$ the set of not yet labeled rectangles (rectangles $R(i)$ with $i < c$). In the sequence $s_1, \ldots, s_k$ of segments forming the boundary between $\mathcal{L}$ and $\mathcal{U}$, let s_i be the one that has $R(d)$ on its left and $R(a)$ on its right when meeting the horizontal axis of $\mathcal{R}$. Since $R(d) \in \mathcal{L}$ and $R(a) \in \mathcal{U}$, s_i has slope $+1$. Let r be the rectangle whose north-tip is the top extremity of s_i. Then r is a maximal element of $\mathcal{U}$ (for the bottom-to-top order) that is weakly to the right of $R(a)$. Since r is left of $R(c)$, the good rectangle $R(c-1)$ at step $c-1$ is weakly to the right of r. Hence $R(c-1)$ is weakly to the right of $R(a)$. But $a < b < c$, so $R(c-1) \neq R(a)$ so $R(c-1)$ is (strictly) to the right of $R(a)$. We conclude that $b, d, a, c-1$ form a forbidden pattern 2–41–3, which is impossible by minimality of c. This is the contradiction.

A symmetric argument shows that there is no pattern 3–14–2. Hence the permutation is Baxter. $\square$

Lemma 6.7. *If at some step of the labeling procedure, the chosen maximal element of $\mathcal{U}$ is not the good rectangle, then the output permutation σ is not Baxter.*

Proof. Consider a labeling scenario (as usual call $R(i)$ the rectangle labeled at step i for each $n \geq i \geq 1$) where at some step k the chosen rectangle $R(k)$ is not the good one, and let $r = R(b)$ be the good rectangle at that step; note that $b < k$ since $R(b)$ will be treated after $R(k)$. Clearly $k < n$ since there is only one choice for $R(n)$ at the first step. Call $\mathcal{L}$ the set of rectangles labeled before step k (rectangles $R(i)$ with $i > k$) and $\mathcal{U}$ the set of rectangles labeled from step k (rectangles $R(i)$ with $i \leq k$). We treat the case where the south tip p of $R(k+1)$ is a $\vee$ (the case $\times$ can be treated similarly).
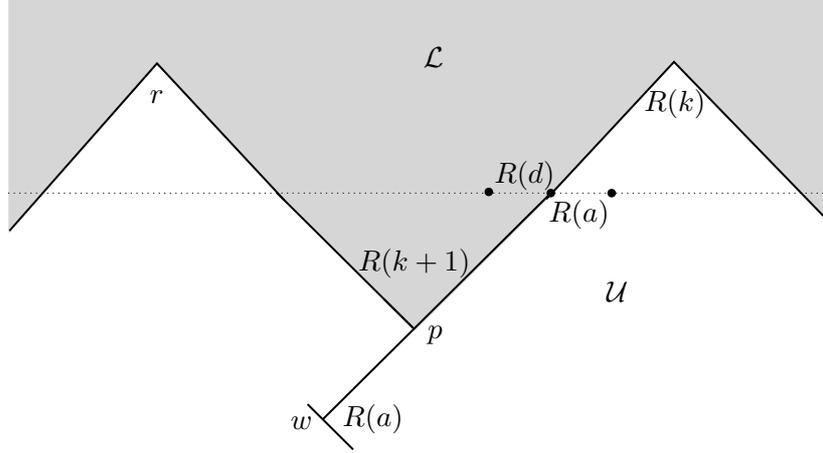

Figure 16: The situation when $R(k)$ is to the right of $R(k+1)$.

First assume that $R(k)$ is to the right of $R(k + 1)$, see Figure 16. Call S the longest segment of slope $+1$ in $\mathcal{R}$ that contains p. At the intersection of S with the horizontal axis of $\mathcal{R}$, let $R(a)$ be the rectangle to the right of S and $R(d)$ the rectangle to the left of S on the horizontal axis. An important observation is that the west-tip w of $R(a)$ is at the bottom end of S (otherwise there would be a rectangle with w as north tip, and this rectangle would be strictly below the horizontal axis of $\mathcal{R}$, which is impossible). Hence, as shown in Figure 16, $R(a)$ is strictly smaller than $r = R(b)$ in the bottom-to-top order, which implies that $a < b$. Hence we have $a < b < k < k + 1 \leq d$ (where $k + 1 \leq d$ because $R(k + 1)$ is the most recently treated element in $\mathcal{L}$); and the left-to-right order of the rectangles is $R(b), R(d), R(a), R(k)$ (see Figure 16), which implies that b, d, a, k form a forbidden pattern 2–41–3.

Now assume that $R(k)$ is to the left of $R(k+1)$, see Figure 17. In the sequence $s_1, \ldots, s_k$ of segments forming the boundary between $\mathcal{U}$ and $\mathcal{L}$, let S be the one of slope $+1$ and with top extremity the north-tip of r. At the intersection between S and the horizontal axis of $\mathcal{R}$, let $R(d)$ be the rectangle to the left of S on the horizontal axis, and $R(a)$ the rectangle to the right of S on the horizontal axis. Note that $R(a) \neq R(k)$ since they have different north-tips. Also $R(k+1) \neq R(d)$ since they have different south-tips. Since $R(k+1)$ is the most recently treated element in $\mathcal{L}$ we have $d > k+1$. Since the first treated element from $\mathcal{U}$ will be $R(k)$ we have $a < k$. Moreover the left-to-right order of these rectangles is $R(k), R(d), R(a), R(k + 1)$ (see Figure 17). Hence $k, d, a, k + 1$ from the forbidden pattern 2–41–3.

Symmetrically one shows that if the south-tip p of $R(k + 1)$ is a $\times$ it yields a forbidden pattern 3–14–2 (again distinguishing whether $R(k)$ is left or right of $R(k + 1)$). $\qquad \square$
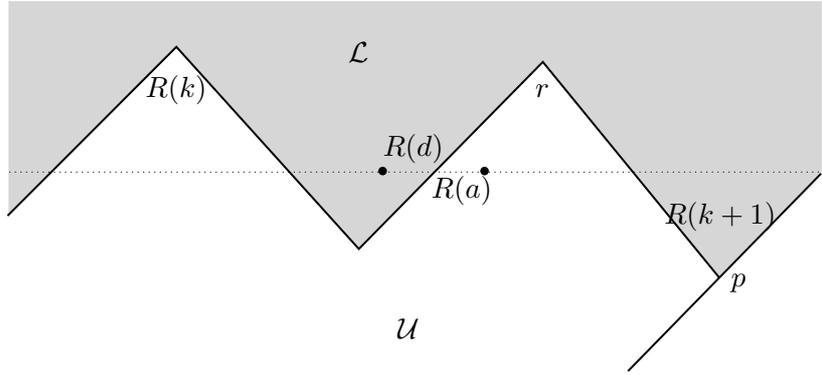
Figure 17: The situation when $R(k)$ is to the left of $R(k+1)$.

Lemmas 6.6 and 6.7 ensure that exactly one admissible permutation is Baxter for every given rectangulation, which concludes the proof of Theorem 6.4. We obtain:

Proposition 6.8. *The number $\Theta_{k,\ell}$ counts*

- *twin pairs of binary trees with $k+1$ left leaves and $\ell+1$ right leaves,*
- *Baxter permutations of $k+\ell+1$ with k descents and ℓ rises.*

Note.

Baxter numbers first appeared in the context of counting Baxter permutations. Chung, Graham, Hoggatt and Kleiman [12] found some interesting recurrences and gave a proof based on generating functions. Mallows [34] found the refined count of Baxter permutations by rises (Proposition 6.8). The bijection of Theorem 6.4 is essentially due to Dulucq and Guibert [18, 19]. Their description and proof, however, does not use geometry. They also prove Proposition 6.8 and some even more refined counts, e.g., the number of Baxter permutations of $[n]$ with ℓ rises and s left-to-right maxima and t right-to-left maxima.

A permutation $(a_1, a_2, \ldots, a_n)$ is *alternating* if $a_1 < a_2 > a_3 < a_4 > \ldots$, i.e., each consecutive   *alternating* pair a_{2i-1}, a_{2i} is a rise and each pair a_{2i}, a_{2i+1} a descent. Alternating permutations are characterized by the property that the reduced fingerprints of their min- and max-trees are alternating, i.e., of the form $\ldots 0, 1, 0, 1, 0, 1, \ldots$ and in addition, to ensure that the first pair is a rise, the first entry of the reduced fingerprints of the max-tree is a 0. Due to this characterization we obtain the following specialization of Theorem 6.4:

Lemma 6.9. *Twin pairs of binary trees with an alternating reduced fingerprint starting with a 0 and alternating Baxter permutations are in bijection.*

Let T be a binary tree with n leaves and with an alternating reduced fingerprint starting with a 0. Note that a 10 subsequence in a fingerprint corresponds to a pair of leaves attached to the same inner node. Thus, the leaves of T (except the last one if n odd) come as pairs of children of inner nodes. Pruning these paired leaves we obtain a tree T' with $n - \lfloor \frac{n}{2} \rfloor$ leaves. From T' we come back to T by attaching a new pair of leaves to each of the first $\lfloor \frac{n}{2} \rfloor$ leaves of T'. Using this kind of correspondence we obtain two bijections (see Figure 18):

- a bijection between alternating Baxter permutations of $[2k-1]$ and pairs of binary trees with k leaves, and

- a bijection between alternating Baxter permutations of $[2k]$ and pairs of binary trees with k and $k + 1$ leaves.

Theorem 6.10. *The number of alternating Baxter permutations on $[n - 1]$ is $C_{k-1}C_k$ if $n = 2k$, and $C_{k-1}C_{k-1}$ if $n = 2k - 1$.*
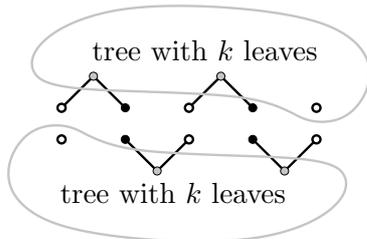
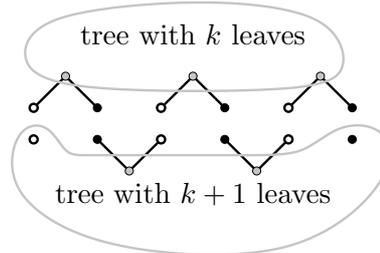The odd case $n = 2k - 1$ The even case $n = 2k$

Figure 18: Alternating Baxter permutations and pairs of trees.

Note.

Theorem 6.10 was obtained by Cori et al. [13]. They gave a nice bijection between alternating Baxter permutations and shuffle of parenthesis systems. The theorem was reproved by Dulucq and Guibert [18] as a specialization of their bijection between Baxter permutations and twin pairs of binary trees. In [28] it is shown that alternating Baxter permutations with the property that their inverse is again alternating Baxter are counted by the Catalan numbers.

In recent work of Bonichon, Bousquet-Mélou and Fusy [8] a direct bijection between Baxter permutations and plane bipolar orientations was given. Their procedure consists in drawing segments in the diagrammatic representation of a Baxter permutation so as to form an embedded plane bipolar orientation.

7 Symmetries

The bijections we have presented have the nice property that they commute with the half-turn rotation, which makes possible to count *symmetric* combinatorial structures. The first structures we have encountered are 2-orientations. Given a 2-orientation O, exchanging the two special vertices $\{s, t\}$ of O clearly yields another 2-orientation, which we call the *pole-inverted* 2-orientation of O and denote by $\iota(O)$. A 2-orientation is called *pole-symmetric* if O and $\iota(O)$ are isomorphic.

Considering the associated separating decomposition, the blue tree of O is the red tree of $\iota(O)$ and vice versa. Accordingly, a 2-orientation is pole-symmetric if, and only if, the blue tree and the red tree are isomorphic as rooted trees, in which case the separating decomposition is called *pole-symmetric* as well. Such a symmetry translates to half-turn rotation symmetries on the associated embeddings. Indeed, as the two trees composing the separating decomposition are isomorphic, so are their alternating embeddings and so are the two binary trees that compose the associated twin pair of binary trees, in which case the twin pair is called *symmetric*. To integrate the main observations:

Lemma 7.1. *A 2-orientation, resp. a separating decomposition, is pole-symmetric if, and only if, the associated twin pair of binary trees is symmetric.*

Clearly, a 2-book embedding and a rectangulation are stable under the half-turn rotation that exchanges the two special vertices, if and only if the corresponding separating decomposition is pole-symmetric.

Considering bipolar orientations, the effect of the half-turn symmetry of a separating decomposition on the associated plane bipolar orientation is clearly that the orientation is unchanged when the poles are exchanged, the directions of all edges are reversed, and the root-edge is flipped to the other side of the outer face (in fact, it is more convenient to forget about the root-edge here). Such bipolar orientations are called *pole-symmetric*.

Lemma 7.2. *A bipolar orientation is pole-symmetric if, and only if, the associated 2-orientation, resp. separating decomposition, is pole-symmetric.*

We next turn to Baxter permutations. Given a permutation π of $1, 2, .., n$ let $\bar{\pi}$ be the permutation obtained by exchanging i with $n - i + 1$ in the one-line representation. A permutation with $\pi = \rho(\bar{\pi})$ is called *symmetric*. Another way to state this is that a permutation π is symmetric if its 0-1 matrix is invariant under half-turn rotation. Consider the rectangulation $R(\pi)$ associated to π as in Section 6. The rectangulation corresponding to $\bar{\pi}$ is obtained from $R(\pi)$ by a reflection along the x-axis. The rectangulation corresponding to $\rho(\pi)$ is obtained from $R(\pi)$ by a reflection along the y-axis. Hence, the rectangulation corresponding to $\rho(\bar{\pi})$ is obtained from $R(\pi)$ by a half-turn rotation. From the bijection between rectangulations and Baxter permutations we thus obtain:

Lemma 7.3. *A Baxter permutation is symmetric if, and only if, the associated rectangulation is invariant under half-turn rotation if, and only if, the associated twin pair of binary trees is symmetric.*
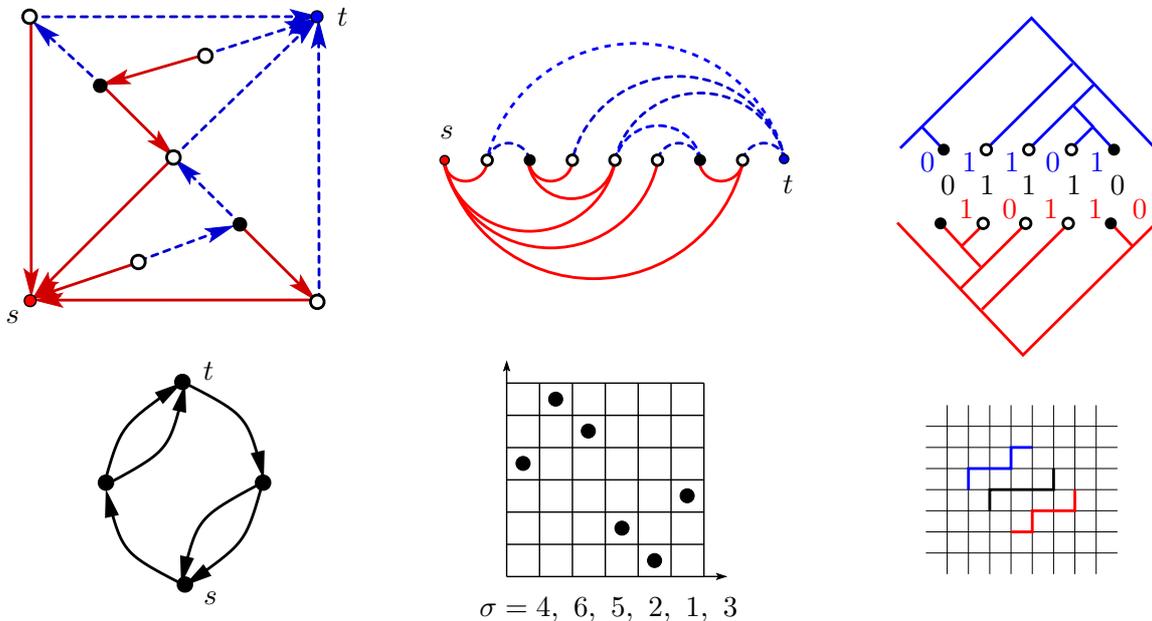

Figure 19: A pole-symmetric separating decomposition and the corresponding symmetric combinatorial structures: 2-book embedding, twin pair of binary trees, plane bipolar orientation, Baxter permutation, triple of paths.

Next we turn to the encoding by a triple of paths. Recall that, in a twin pair (T, T') of binary trees, the reduced fingerprints satisfy the relation $\hat{\alpha}(T) = \rho(\hat{\alpha}(T'))$. Hence, a symmetric twin pair (T, T) has the property that the reduced fingerprint of T satisfies $\hat{\alpha}(T) = \rho(\hat{\alpha}(T))$, i.e., $\hat{\alpha}$ is a palindrome. Equivalently, if T has $k+1$ left leaves and $\ell+1$ right leaves, the up-right lattice path $P_2 = P_\alpha(T)$ from $(1, 1)$ to $(k+1, \ell+1)$, as defined in Section 5, is stable under the point-reflection π_S at $S := (k/2 + 1, \ell/2 + 1)$. The other two paths in the triple (P_1, P_2, P_3) of non-intersecting lattice paths correspond to two copies of the bodyprint of T read respectively from $(0, 2)$ to $(k, \ell + 2)$ for P_1 and from $(\ell + 2, k)$ to $(2, 0)$ for P_3. Therefore the whole triple (P_1, P_2, P_3) is stable under the point reflection π_S. Such a triple of paths is called *symmetric*. We have:

Lemma 7.4. *A triple (P_1, P_2, P_3) of paths is symmetric if, and only if, the associated twin pair of binary trees is symmetric.*

Proposition 7.5. *Let $\Theta_{k,\ell}^{\circlearrowleft}$ be the number of symmetric non-intersecting triples of up-right lattice paths (P_1, P_2, P_3) going respectively from $(0, 2)$, $(1, 1)$, $(2, 0)$ to $(k, \ell + 2)$, $(k + 1, \ell + 1)$, $(k + 2, \ell)$.*
   (i) If k and ℓ are odd, then $\Theta_{k,\ell}^{\circlearrowleft} = 0$.
   (ii) If k and ℓ are even, $k = 2\kappa$, $\ell = 2\lambda$, then

$$\Theta_{k,\ell}^{\circlearrowleft} = \sum_{r \geq 1} \frac{2r^3}{(\kappa + \lambda + 1)(\kappa + \lambda + 2)^2} \binom{\kappa + \lambda + 2}{\kappa + 1} \binom{\kappa + \lambda + 2}{\kappa - r + 1} \binom{\kappa + \lambda + 2}{\kappa + r + 1}.$$

   (iii) If k is odd and ℓ is even, $k = 2\kappa + 1$, $\ell = 2\lambda$, then

$$\Theta_{k,\ell}^{\circlearrowleft} = \sum_{r \geq 1} \frac{2r^3 + (\lambda - r + 1)r(r + 1)(2r + 1)}{(\kappa + \lambda + 1)(\kappa + \lambda + 2)^2} \binom{\kappa + \lambda + 2}{\kappa + 1} \binom{\kappa + \lambda + 2}{\kappa - r + 1} \binom{\kappa + \lambda + 2}{\kappa + r + 1}.$$

   (iv) If k is even and ℓ is odd, $k = 2\kappa$, $\ell = 2\lambda + 1$, then

$$\Theta_{k,\ell}^{\circlearrowleft} = \sum_{r \geq 1} \frac{2r^3 + (\kappa - r + 1)r(r + 1)(2r + 1)}{(\kappa + \lambda + 1)(\kappa + \lambda + 2)^2} \binom{\kappa + \lambda + 2}{\kappa + 1} \binom{\kappa + \lambda + 2}{\kappa - r + 1} \binom{\kappa + \lambda + 2}{\kappa + r + 1}.$$

Proof. By definition, (P_1, P_2, P_3) is stable under the point-reflection π_S at $S := (\ell/2 + 1, k/2 + 1)$. In particular, P_2 is stable under π_S, so that P_2 has to pass by S. This can only occur if S is on an axis-coordinate, i.e., $k/2$ or $\ell/2$ are integers. Therefore $\Theta_{k,\ell}^{\circlearrowleft} = 0$ if both k and ℓ are odd.

If k and ℓ are even, $k = 2\kappa$ and $\ell = 2\lambda$, the half-turn symmetry ensures that (P_1, P_2, P_3) is completely encoded upon keeping the part P_1', P_2', P_3' of the paths that lie in the half-plane $\{x + y \leq x_S + y_S\}$, i.e., the half-plane $\{x + y \leq \kappa + \lambda + 2\}$. The conditions on (P_1, P_2, P_3) translate to the following conditions on the reduced triple: (P_1', P_2', P_3') is non-intersecting, has same starting points as (P_1, P_2, P_3), the endpoint of P_2' is S, and the endpoints of P_1' and P_3' are equidistant from S, i.e., there exists an integer $r \geq 1$ such that P_1' ends at $(\kappa + 1 - r, \lambda + 1 + r)$ and P_3' ends at $(\kappa + 1 + r, \lambda + 1 - r)$. Hence, up to fixing $r \geq 1$, (P_1', P_2', P_3') form a non-intersecting triple with explicit fixed endpoints, so that the number of such triples can be expressed using Lindström Gessel-Viennot determinant formula. The expression for $\Theta_{k,\ell}^{\circlearrowleft}$ follows.

If k is odd and ℓ is even, $k = 2\kappa + 1$ and $\ell = 2\lambda$, the triple (P_1, P_2, P_3) is again completely encoded by keeping the part (P_1', P_2', P_3') of the paths that lie in $\{x + y \leq x_S + y_S\}$, i.e., the

half-plane $\{x + y \leq \kappa + \lambda + 5/2\}$. The difference with the case where k and ℓ are even is that P_1', P_2', P_3' are not standard lattice paths, as they end with a step of length $1/2$. Similarly as before, the conditions on (P_1, P_2, P_3) are equivalent to the properties that (P_1', P_2', P_3') are non-intersecting, have the same starting points as (P_1, P_2, P_3), P_2' ends at S, and P_1', P_3' end at points that are equidistant from S on the line $\{x + y = x_S + y_S\}$ and have one integer coordinate, i.e., there exists an integer $m \geq 2$ such that P_1' ends at $(x_S - m/2, y_S + m/2)$ and P_3' ends at $(x_S + m/2, y_S - m/2)$. Notice that, upon discarding the last step, the system (P_1', P_2', P_3') is equivalent to a triple of non-intersecting up-right lattice paths $(\overline{P_1'}, \overline{P_2'}, \overline{P_3'})$ with starting points $(0, 2)$, $(1, 1)$, $(2, 0)$, and endpoints that are either of the form $(\kappa+1-r, \lambda+1+r)$, $(\kappa+1, \lambda+1)$, $(\kappa+1+r, \lambda+1-r)$ if m is even, $m = 2r$, or are of the form $(\kappa+1-r, \lambda+1+r)$, $(\kappa + 1, \lambda + 1)$, $(\kappa + 2 + r, \lambda - r)$ if m is odd, $m = 2r + 1$. In each case, the number of triples has an explicit form from the formula of Lindström Gessel-Viennot. The expression of $\Theta_{k,\ell}^{\circlearrowleft}$ follows. Finally, notice that the set of symmetric non-intersecting triples is stable under swapping x-coordinates and y-coordinates, yielding the relation $\Theta_{k,\ell}^{\circlearrowleft} = \Theta_{\ell,k}^{\circlearrowleft}$. Thus the formula for $\Theta_{k,\ell}^{\circlearrowleft}$ when k is even and ℓ is odd simply follows from the formula obtained when k is odd and ℓ is even. $\qquad\square$

The whole discussion on symmetric structures is summarized in the following proposition and illustrated in Figure 19.

Theorem 7.6. *The number $\Theta_{k,\ell}^{\circlearrowleft}$ counts*

- *pole-symmetric 2-orientations with $k + 1$ white vertices and $\ell + 1$ black vertices,*

- *pole-symmetric separating decompositions and 2-book embeddings with $k + 1$ white vertices and $\ell + 1$ black vertices,*

- *symmetric twin pairs of binary trees with $k + 1$ left leaves and $\ell + 1$ right leaves,*

- *rectangulations of X_n with k horizontal and ℓ vertical segments, which are invariant under half-turn rotation,*

- *symmetric Baxter permutations of $k + \ell + 1$ with k descents and ℓ rises,*

- *pole-symmetric plane bipolar orientations with k inner faces and ℓ non-pole vertices.*

8 Schnyder Families

As we have shown in previous sections, Baxter numbers count 2-orientations on quadrangulations and several other structures. We now turn to a family of structures, Schnyder woods, which are equinumerous with 3-orientations of plane triangulations. Actually, the relation of Schnyder woods and 3-orientations is very similar to the relation of separating decompositions and 2-orientations. In both cases the coloring of an edge in the richer structure can be recovered by following a unique path that leads to one of the special vertices, see Theorems 8.3 and 2.5.

Consider a plane triangulation T, i.e., a maximal plane graph, with n vertices and three special vertices a_1, a_2, a_3 in clockwise order around the outer face.

Definition 8.1. An orientation and coloring of the inner edges of T with colors red, green and blue is a *Schnyder wood* if:

(1) All edges incident to a_1 are ingoing red, all edges incident to a_2 are ingoing green and all edges incident to a_3 are ingoing blue.

(2) Every inner vertex v has three outgoing edges colored red, green and blue in clockwise order. All the incoming edges in an interval between two outgoing edges are colored with the third color; see Figure 20.
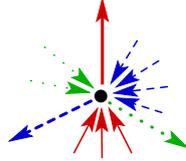
Figure 20: Schnyder's edge coloring rule.

Definition 8.2. An orientation of the inner edges of T is a *3-orientation* if every inner vertex has outdegree three.

From the count of edges it follows that the special vertices a_i are sinks in every 3-orientation. Clearly, forgetting the colors of edges in a Schnyder wood yields a 3-orientation. In the next theorem it is shown that the two structures are actually equivalent. This resembles the equivalence between separating decompositions and 2-orientations described in Theorem 2.5.

Theorem 8.3 (de Fraysseix and de Mendez [14])**.** *Let T be a plane triangulation with outer vertices a_1, a_2, a_3. Schnyder woods and 3-orientations of T are in bijection.*

Given an edge e which is incoming at v, we can classify the outgoing edges at v as left, straight and right. Define the *straight-path* of an edge as the path which always takes the straight outgoing edge. A count and Euler's formula shows that every straight-path ends in a special vertex. The special vertex where a straight-path ends determines the color of all the edges along the path. It can also be shown that two straight-paths starting at a vertex do not meet again. This implies that the coloring of the orientation is a Schnyder wood.

From this proof it follows that the local properties (1) and (2) of Schnyder woods imply:

(3) *The edges of each color form a tree rooted at a special vertex and spanning all the inner vertices.*

Recall that in the case of separating decompositions we also found the tree decomposition being implied by local conditions (see item (3) after Theorem 2.5).

Note.

Schnyder woods were introduced by Schnyder in [39] and [40]. They have numerous applications in the context of graph drawing, e.g., [3, 7, 32], dimension theory for orders, graphs and polytopes, e.g., [39, 9, 21], enumeration and encoding of planar structures, e.g., [36, 24]. The connection with 3-orientations was found by de Fraysseix and Ossona de Mendez [14].

The aim of this section is to prove the following theorem of Bonichon.

Theorem 8.4 (Bonichon [6])**.** *The total number of Schnyder woods on triangulations with* $n + 3$ *vertices is*

$$V_n = C_{n+2}\, C_n - C_{n+1}^2 = \frac{6\,(2n)!\,(2n+2)!}{n!\,(n+1)!\,(n+2)!\,(n+3)!}$$

where $C_n = \frac{1}{n+1}\binom{2n}{n}$ *is the Catalan number.*

Before going into details we outline the proof. We first show a bijection between Schnyder woods and a special class of bipolar orientations of plane maps. We trace these bipolar orientations through the bijection with separating decompositions, twin pairs of trees and triples of non-intersecting paths. Two of the three paths turn out to be equal and the remaining pair is a non-crossing pair of Dyck paths. This implies the formula.

Note.

The original proof, Bonichon [6], and a more recent simplified version, Bernardi and Bonichon [5], are also based on a bijection between Schnyder woods and pairs of non-crossing Dyck paths. In [5] the authors also enumerate special classes of Schnyder woods. Fusy, Schaeffer and Poulalhon have a bijection from Schnyder woods to a special class of separating decompositions and a bijection from these separating decompositions to pairs of non-crossing Dyck paths. They show that their bijection equals the bijection from [5]. Our proof yields a different bijection.

Little is known about the number of Schnyder woods of a fixed triangulation. In [22] it is shown that the maximal number of Schnyder woods a triangulation on n vertices can have is asymptotically between $2,37^n$ and $3,56^n$. As with 2-orientations, the computational complexity of the counting problem is unknown.

Recall that by Fact F, after Definition 2.2, the boundary of every inner face of a planar bipolar orientation consists of two directed paths starting at the face-source and joining at the face-sink. The *right side* of the face is the right of the two paths when looking from the face-source to the interior of the face.

Proposition 8.5. *There is a bijection between Schnyder woods on triangulations with* $n + 3$ *vertices and plane bipolar orientations with* $n + 2$ *vertices having the special property:*

$(\star)$ *The right side of every bounded face is of length two.*

Proof. Let T be a triangulation with a Schnyder wood S. With (T, S) we associate a pair (M, B), where M is a subgraph of T and B a bipolar orientation on M. The construction is in two steps. First, we delete from the graph the edges of the green tree in S and the special vertex of that tree, i.e., a_2, as well as the two outer edges incident to a_2. The resulting map is M. Then we revert the orientation of all blue edges and orient the edge $\{a_3, a_1\}$ from a_3 to a_1, this is the orientation B. Figure 21 shows an example.

The orientation B has a_3 as unique source and a_1 as unique sink. To show that it is bipolar it is enough to verify properties V and F (c.f. the note after Proposition 2.3). Property V requires that at a vertex $v \neq s, t$ the edges partition into nonempty intervals of incoming and outgoing edges, this is immediate from the edge coloring rule (2) in Definition 8.1 and the construction of B.

For Property F, consider a bounded face f of M. Suppose that f is of degree > 3, then there had been some green edges triangulating the interior of f. The coloring rule for the
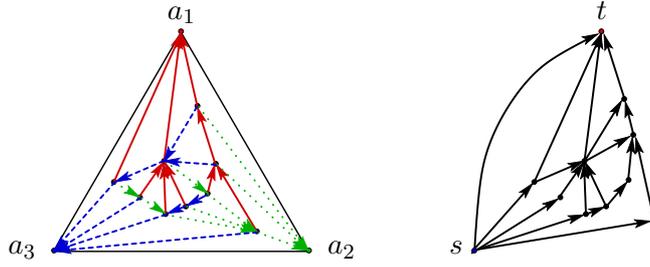
Figure 21: A Schnyder wood and the corresponding bipolar orientation.

vertices on the boundary of f implies that these green edges form a fan, as indicated in Figure 22. Otherwise there would be a vertex with two outgoing green edges or a vertex with adjacent incoming and outgoing green edges; both are impossible. Starting from the green edges, we conclude that each edge on the left side of f is red and upward pointing or blue and downward pointing. Hence, in B these edges form a directed path and the neighbors of the tip vertex of the green edges are the unique source and sink of f. This also implies that the right side of f is of length two, i.e., property $(\star)$.

If f is a triangle, then two of its edges are of the same color, say red. The coloring rule implies that these two edges point to their common vertex, whence the triangle has unique source and sink. Since the transitive vertex of f has a green outgoing edge in S, it is on the right side and $(\star)$ also holds for f.
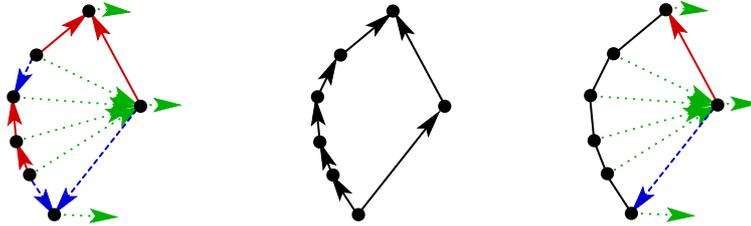

Figure 22: From a generic face in S to B and back.

For the converse mapping, consider a pair (M, B) such that $(\star)$ holds. From Property V it follows that every vertex $v \neq s, t$ has a unique face where it belongs to the right side. This allows us to identify the red and the blue outgoing edges of v. Since every edge except the (s, t) edge is on the right side of some face, the procedure determines a color for all these edges. Moreover, at v the leftmost incoming edge is blue and all the other incoming edges are red. The coloring of outgoing edges at v is dual, the leftmost is red and all the others are blue. Insert the green edges so that they triangulate faces of degree more than three and connect vertices on the rightmost s-t path to the additional outer vertex a_2. The green edges form a tree rooted at a_2. Finally, revert the orientation of the blue edges. This yields a coloring and orientation of the edges of the triangulation obeying properties (1) and (2) from Definition 8.1. Hence, we could reconstruct the unique Schnyder wood compatible with the data given by (M, B). This proves the bijection. □

Given a plane bipolar orientation (M, B) with $n + 2$ vertices and the $(\star)$ property, we apply the bijection from Proposition 2.3 to obtain a quadrangulation Q with a separating decomposition. Property $(\star)$ in (M, B) is equivalent in Q to

29

($\star'$) Every white vertex (except the rightmost one) has a unique incoming edge in the blue tree.

In particular, it follows that there is a matching between vertices $v \neq s, t$ and bounded faces of M, hence, in Q there are $n + 2$ black and $n + 1$ white vertices.

The separating decomposition of Q yields twin pairs of alternating trees with $n + 1$ black and n white vertices (Theorem 3.6). From the twin pair of alternating trees we get to a pair of twin binary trees with $n + 1$ black and n white vertices (Theorem 5.2). This pair of trees yields a triple of non-intersecting paths (Theorem 5.5). Figure 23 shows an example of the sequence of transformations.
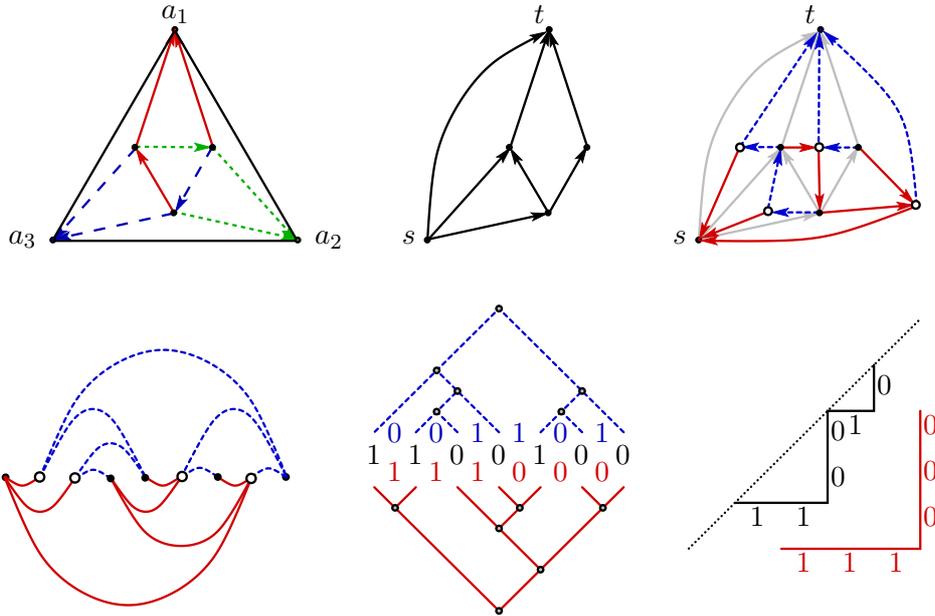

Figure 23: From a Schnyder wood to a pair of non-intersecting Dyck-paths..

From ($\star'$) we get some crucial properties of the fingerprint and the bodyprints of the blue tree T^b and the red tree T^r.

Fact 1. If we add a leading 1 to the reduced fingerprint $\hat{\alpha}$, then we obtain a Dyck word; in symbols $(10)^n \leq_{\mathsf{dom}} 1 + \hat{\alpha}$.

Proof. It is better to think of $1 + \hat{\alpha}$ as the fingerprint α^b of the blue tree after removal of the last 0. Property ($\star'$) implies that there is a matching between all 1's and all but the last 0's in the α^b, such that each 1 is matched to a 0 further to the right. $\triangle$

Fact 2. The fingerprint uniquely determines the bodyprint of the blue tree, precisely $\overline{\beta^b} = 1 + \hat{\alpha}$.

Proof. From ($\star'$) it follows that $\alpha_i^b = 1$ implies $\beta_{i+1}^b = 0$. Since α^b has n entries 1 and β^b has this same number of 0's, it follows that β^b is determined by α^b. $\triangle$

Let $\alpha^* = 1 + \hat{\alpha}$ and $\beta^* = 1 + \hat{\beta}^r$; then $(10)^n \leq_{\mathsf{dom}} \alpha^* \leq_{\mathsf{dom}} \beta^*$. We omit the proof that actually every pair (α^*, β^*) of 0,1 strings from $\left\langle {2n \atop n} \right\rangle$ with these properties comes from a unique Schnyder wood on a triangulation with $n + 3$ vertices. Translating the resulting bijection with strings into the language of paths we obtain:

Theorem 8.6. *There is a bijection between Schnyder woods on triangulations with $n + 3$ vertices and pairs (P_1, P_2) of non-intersecting up-right lattice paths, where P_1 is from $(0,0)$ to (n,n), P_2 is from $(1,-1)$ to $(n+1, n-1)$, and the paths stay weakly below the diagonal, i.e., they avoid all points (x, y) with $y > x$.*

For the actual counting of Schnyder woods we again apply the Lemma of Lindström Gessel-Viennot. The entry $A_{i,j}$ in the matrix is the number of paths from the start of P_i to the end of P_j staying weakly below the diagonal. The reflection principle of D. André allows us to write these numbers as differences of binomials.

Proposition 8.7. *The number of Schnyder woods on triangulations with $n + 3$ vertices is*

$$\det \begin{pmatrix} \binom{2n}{n} - \binom{2n}{n-1} & \binom{2n}{n+1} - \binom{2n}{n-2} \\ \binom{2n}{n-1} - \binom{2n}{n-2} & \binom{2n}{n} - \binom{2n}{n-3} \end{pmatrix} = \frac{6\,(2n)!\,(2n+2)!}{n!\,(n+1)!\,(n+2)!\,(n+3)!}$$

Acknowledgements. Mireille Bousquet-Mélou and Nicolas Bonichon are greatly thanked for fruitful discussions. We also thank an anonymous referee whose recommendations helped to improve the exposition.

References

[1] E. ACKERMAN, G. BAREQUET, AND R. PINTER, *On the number of rectangulations of a planar point set*, J. Combin. Theory Ser. A, 113 (2006), pp. 1072–1091.

[2] M. AIGNER, *A Course in Enumeration*, vol. 238 of Graduate Texts in Mathematics, Springer-Verlag, 2007.

[3] I. BÁRÁNY AND G. ROTE, *Strictly convex drawings of planar graphs*, Documenta Math., 11 (2006), pp. 369–391.

[4] R. J. BAXTER, *Dichromatic polynomials and Potts models summed over rooted maps*, Annals of Combinatorics, 5 (2001), p. 17.

[5] O. BERNARDI AND N. BONICHON, *Intervals in Catalan lattices and realizers of triangulations*, J. Combin. Theory Ser. A, 116:1 (2009), pp. 55–75.

[6] N. BONICHON, *A bijection between realizers of maximal plane graphs and pairs of non-crossing Dyck paths*, Discrete Math., 298 (2005), pp. 104–114.

[7] N. BONICHON, S. FELSNER, AND M. MOSBAH, *Convex drawings of 3-connected planar graphs*, Algorithmica, 47 (2007), pp. 399–420.

[8] N. BONICHON, M. BOUSQUET-MÉLOU AND É. FUSY, *Baxter permutations and plane bipolar orientations*, Séminaire Lotharingien de Combinatoire 61A (2010), Article B61Ah, 29 pages.

[9] G. BRIGHTWELL AND W. T. TROTTER, *The order dimension of convex polytopes*, SIAM J. Discrete Math., 6 (1993), pp. 230–245.

[10] T. BRYLAWSKI AND J. OXLEY, *The Tutte polynomial and its applications*, in Matroid Applications, Cambr. Univ. Press, 1992, pp. 123–225.

[11] N. CHIBA, T. NISHIZEKI, S. ABE, AND T. OZAWA, *A linear algorithm for embedding planar graphs using PQ-trees*, J. Comput. Syst. Sci., 30(1) (1985), pp. 54–76.

[12] F. Chung, R. Graham, V. Hoggatt, and M. Kleiman, *The number of Baxter permutations*, J. Combin. Theory, Ser. A, 24 (1978), pp. 382–394.

[13] R. Cori, S. Dulucq, and G. Viennot, *Shuffle of pharentesis systems and Baxter permutations*, J. Combin. Theory Ser. A, 43 (1986), pp. 1–22.

[14] H. de Fraysseix and P. O. de Mendez, *On topological aspects of orientation*, Discrete Math., 229 (2001), pp. 57–72.

[15] H. de Fraysseix, P. O. de Mendez, and J. Pach, *A left-first search algorithm for planar graphs*, Discrete Comput. Geom., 13 (1995), pp. 459–468.

[16] H. de Fraysseix, P. Ossona de Mendez, and P. Rosenstiehl, *Bipolar orientations revisited*, Discrete Appl. Math., 56 (1995), pp. 157–179.

[17] P. O. de Mendez, *Orientations bipolaires*, PhD thesis, École des Hautes Études en Sciences Sociales, Paris, 1994.

[18] S. Dulucq and O. Guibert, *Stack words, standard tableaux and Baxter permutations*, Discrete Math., 157 (1996), pp. 91–106.

[19] S. Dulucq and O. Guibert, *Baxter permutations*, Discrete Math., 180 (1998), pp. 143–156.

[20] S. Felsner, C. Huemer, S. Kappes, and D. Orden, *Binary labelings for plane quadrangulations and their relatives*. `arXiv:math.CO/0612021`, 2007.

[21] S. Felsner and S. Kappes, *Orthogonal surfaces and their CP-orders*, Order, 25 (2008), pp. 19–47.

[22] S. Felsner and F. Zickfeld, *On the number of planar orientations with prescribed degrees.* Electron. J. Combin. 15, (2008) R77, 41 p.

[23] É. Fusy, *Straight-line drawing of quadrangulations*, in Proceedings of Graph Drawing '06, vol. 4372 of LNCS, 2007, pp. 234–239.

[24] É. Fusy, D. Poulalhon, and G.Schaeffer, *Dissections, orientations, and trees, with applications to optimal mesh encoding and to random sampling*, Transactions on Algorithms, 4 (2008), Art. 19.

[25] É. Fusy, D. Poulalhon, and G. Schaeffer, *Bijective counting of plane bipolar orientations and Schnyder woods*, Europ. J. Combin. 30, (2009), pp. 1646–1658.

[26] I. Gelfand, M. Graev, and A. Postnikov, *Combinatorics of hypergeometric functions associated with positive roots*, in The Arnold-Gelfand Mathematical Seminars: Geometry and Singularity Theory, V.I. Arnold, ed., Birkhäuser, 1997, pp. 205–221.

[27] I. Gessel and G. Viennot, *Binomial determinants, paths, and hook length formulae*, Adv. Math., 58 (1985), pp. 300–321.

[28] O. Guibert and S. Linusson, *Doubly alternating Baxter permutations are Catalan*, Discrete Math., 217 (2000), pp. 157–166.

[29] I. B.-H. Hartman, I. Newman, and R. Ziv, *On grid intersection graphs*, Discrete Math., 87 (1991), pp. 41–52.

[30] G. Kant and X. He, *Regular edge labeling of 4-connected plane graphs and its applications in graph drawing problems*, Theoret. Comput. Sci., 172 (1997), pp. 175–193.

[31] A. Lempel, S. Even, and I. Cederbaum, *An algorithm for planarity testing of graphs*, in Theory of Graphs, Int. Symp (New York), 1967, pp. 215–232.

[32] C. Lin, H. Lu, and I.-F. Sun, *Improved compact visibility representation of planar graphs via Schnyder's realizer*, SIAM J. Discrete Math., 18 (2004), pp. 19–29.

[33] P.A. MacMahon, *Combinatorial Analysis, Vols. 1 and 2*, Camb. Univ. Press, 1915; (reprinted by Chelsea, 1960).

[34] C. Mallows, *Baxter permutations rise again*, J. Combin. Theory Ser. A, 27 (1979), pp. 394–396.

[35] T.V. Narayana, *Sur les treillis formés par les partitions d'une unties et leurs applications á la théorie des probabilités*, Comp. Rend. Acad. Sci. Paris 240 (1955), pp. 1188–1189.

[36] D. Poulalhon and G. Schaeffer, *Optimal Coding and Sampling of Triangulations*, Algorithmica 46:3-4, 2006, pp. 505–527.

[37] P. Rosenstiehl and R. E. Tarjan, *Rectilinear planar layouts and bipolar orientations of planar graphs*, Discrete Comput. Geom., 1(4) (1986), pp. 343–353.

[38] G. Rote, I. Streinu, and F. Santos, *Expansive motions and the polytope of pointed pseudo-triangulations*, in Discrete Comput. Geom., The Goodman and Pollack Festschrift, Springer, 2003, pp. 699–736.

[39] W. Schnyder, *Planar graphs and poset dimension*, Order, 5 (1989), pp. 323–343.

[40] W. Schnyder, *Embedding planar graphs on the grid*, in Proc. 1st ACM-SIAM Symp. Discr. Algo., 1990, pp. 138–148.

[41] N. J. A. Sloane, *The on-line encyclopedia of integer sequences*. `http://www.research.att.com/~njas/sequences`.

[42] R. P. Stanley, *Enumerative Combinatorics*, vol. 2, Cambridge Univ. Press, 1999.

[43] R. Tamassia and I. G. Tollis, *A unified approach to visibility representations of planar graphs*, Discrete Comput. Geom., 1(4) (1986), pp. 321–341.

[44] R. Tamassia and I. G. Tollis, *Planar grid embedding in linear time*, IEEE Trans. on Circuits and Systems, CAS-36(9) (1989), pp. 1230–1234.

[45] M. Yannakakis, *Embedding planar graphs in four pages*, J. Comput. System Sci., 38 (1986), pp. 36–67.